Seasonal and depth variations in molecular and isotopic alkenone composition of sinking particles from the western North Pacific

Masanobu Yamamoto[1,*], Akifumi Shimamoto[2], Tatsuo Fukuhara[2], Hiroshi Naraoka[3], Yuichiro Tanaka[4] and Akira Nishimura[4]

[1]Faculty of Environmental Earth Science, Hokkaido University, Sapporo 060-0810, Japan.

[2]The General Environmental Technos Co., LTD., Osaka 541-0052, Japan.

[3]Department of Earth Sciences, Okayama University, Okayama 700-8530, Japan.

[4]National Institute of Advanced Industrial Science and Technology, Tsukuba, Ibaraki 305-8567, Japan

*Corresponding author; myama@ees.hokudai.ac.jp

Abstract:

Seasonal and depth variations in alkenone flux and molecular and isotopic composition of sinking particles were examined using a 21-month time-series sediment trap experiment at a mooring station WCT-2 (39°N, 147°E) in the mid-latitude NW Pacific to assess the influences of seasonality, production depth, and degradation in the water column on the alkenone unsaturation index $U^{K'}_{37}$. Analysis of the underlying sediments was also conducted to evaluate the effects of alkenone degradation at the

water-sediment interface on $U^{K'}_{37}$. Alkenone sinking flux and $U^{K'}_{37}$–based temperature showed strong seasonal variability. Alkenone fluxes were higher from spring to fall than they were from fall to spring. During periods of high alkenone flux, the $U^{K'}_{37}$–based temperatures were lower than the contemporary SSTs, suggesting alkenone production in a well-developed thermocline (shallower than 30m). During low alkenone flux periods, the $U^{K'}_{37}$–based temperatures were nearly constant and were higher than the contemporary SSTs. The nearly constant carbon isotopic ratios of $C_{37:2}$ and $C_{38:2}$ alkenones suggest that alkenones produced in early fall were suspended in the surface water until sinking. The alkenone sinking flux decreased exponentially with increasing depth. The decreasing trend was enhanced during the periods of high alkenone flux, suggesting that fresh and labile particles sank from spring to fall, while old and stable particles sank from fall to spring. The $U^{K'}_{37}$–based temperature usually increased with increasing depth. The preservation efficiency of alkenones was ~2.7–5.2% at the water-sediment interface. Despite the significant degradation of the alkenones, there was little difference in $U^{K'}_{37}$ levels between sinking particles and the surface sediment.

Keywords: alkenones, unsaturation index, sediment trap, the North Pacific, carbon isotopes.

1. Introduction

Long-chain alkenones are biolipids in a specific group of haptophyte algae (Volkman et al., 1980), and until now, they have been reported solely from *Emiliania* and *Gephyrocapsa* (Family Gephyrocapsae) and *Chrysotila* and *Isochrysis* (Family Isochrysidaceae) (Marlowe et al., 1984; Volkman et al., 1995). In open marine

environments, alkenones are thought to be produced exclusively by *Emiliania* and *Gephyrocapsa* (Marlowe et al., 1984; 1990).

Alkenone paleothermometry was proposed in the mid-1980s (Brassell et al., 1986; Prahl and Wakeham, 1987) and has been widely applied to the assessment of late Quaternary changes in sea surface temperatures (reviewed by Brassell, 1993; Müller et al., 1998). Alkenone paleothermometry uses the physiological response of the unsaturation degree of C_{37} alkenones (expressed as U^{K}_{37} and $U^{K'}_{37}$) to the growth temperature. An early attempt exhibited a linear relationship between alkenone unsaturation indices and growth temperature in a batch culture experiment with an *E. huxleyi* strain (55a) from the NE Pacific (Prahl and Wakeham, 1987; Prahl et al., 1988). Nearly identical relationships were found in a comparison of the $U^{K'}_{37}$ of core-top and surface sediments with the mean annual temperature at 0 m in the overlying waters (e.g., Müller et al., 1998; Conte et al., 2006). The calibration equations based on these relationships have been used for assessing sea-surface paleotemperature. Recently Conte et al. (2006) showed that the surface sediment calibration differs significantly from the surface-water calibration and attributed the deviation to the combined effects of seasonality and thermocline production as well as the differential degradation of tri- and di-unsaturated alkenones.

The season and depth of alkenone production determine the value of sedimentary $U^{K'}_{37}$. It is thus necessary to evaluate the effects of these factors on paleotemperature estimation. Because the alkenones sampled by time-series sediment traps record the temperature when and where the alkenones were produced, the temperatures indicated by trapped alkenones provide a key for estimating the season and depth of alkenone production. In the northwestern Pacific, Sawada et al. (1998) reported that the

$U^{K'}_{37}$–based temperatures in sinking particles corresponded with the sea-surface temperatures (SSTs) 1–2 months prior to sampling at the southern margin of the Kuroshio–Oyashio mixing zone. Ohkouchi et al. (1999) argued that alkenones record the temperatures within or below the thermocline (~150 m deep) because the alkenone temperatures in surface sediments were nearly 10°C lower than annual mean SSTs in the overlying water in the subtropical Pacific. In the subarctic Pacific, Harada et al. (2006) reported that $U^{K'}_{37}$–based temperatures in sinking particles corresponded with the thermocline temperatures during the high export season, while they were higher than SSTs during the low export season.

Degradation of alkenones through water and sediment columns presumably affects the alkenone unsaturation index (Freeman and Wakeham, 1992; Hoefs et al., 1998; Gong et al., 1999). If this effect is relatively large, it introduces error into paleotemperature estimations that are based on the alkenone unsaturation index. Alkenone degradation through the water column is evaluated based on the decreasing trend of sinking flux with increasing depth (Müller and Fischer, 2001). Most sediment trap studies, however, have not detected this decreasing trend because of interference by the lateral influx of allochthonous alkenones to deeper traps (e.g., Sawada et al., 1998). Also, very little is known about the degradation rate of alkenones at the water-sediment interface, except for a few studies (e.g., Prahl et al., 1993; Müller and Fischer, 2001). Evaluation requires a combined data set of the sinking fluxes of alkenones through the water column and their accumulation rates in the sediment at the same location.

Lateral advection of allochthonous alkenones by strong surface currents can also alter the alkenone signal. High $U^{K'}_{37}$–based temperature in the southern Indian Ocean during the last glacial maximum has been interpreted as the lateral advection of

warm-water detrital alkenones by the Agulhas Current (Sicre et al., 2005). Other research has attributed the low $U^{K'}_{37}$–based temperature of the suspended particulates in the Brazil-Malvinas Confluence to the lateral advection of cold-water detrial alkenones by the Malvinas Current (Rühlemann and Butzin, 2006; Conte et al., 2006).

In this study, we examined the seasonal and depth variations in alkenone flux and molecular and isotopic compositions of sinking particles using a time-series sediment trap experiment at a selected mooring station (39°N, 147°E; Fig. 1) in the mid-latitude NW Pacific to assess the influences of seasonality, production depth and degradation of alkenones in the water column on $U^{K'}_{37}$. Analysis of the underlying sediments was also conducted to evaluate the effects of alkenone degradation at the water-sediment interface on $U^{K'}_{37}$.

The study site, station WCT-2, is located in the mixing zone between Oyashio and Kuroshio waters (Fig. 1). Cold and warm mesoscale eddies from the Oyashio and Kuroshio, respectively, develop in the mixing zone. The Oyashio–Kuroshio boundary is displaced seasonally. The southern limit of the Oyashio stays at ~38.5°N in April, gradually shifts northward to ~40°N until October, and then moves more rapidly northward to ~41.5°N to December before gradually returning southward until April (Data from Japan Meteorological Agency, http://www.data.kishou.go.jp/kaiyou/db/hakodate/knowledge/oyashio.html.) The monthly mean SST ranges from ~9°C (March) to ~24°C (August) and averages ~15°C (Fig. 2a; Conkright et al., 2002). The seasonal SST change reflects both the latitudinal displacement of the Oyashio–Kuroshio boundary and the development of thermal stratification. Thermal stratification develops from summer to fall in this region (Fig. 2b). An ocean general circulation model study indicated that the average surface current velocity was ~10 cm/sec (~8.6 km/day and

~260 km/month) during winters at site WCT-2 (Nonaka et al., 2006); this velocity is much lower than that of the Kuroshio Extension.

2. Samples and methods

Samples

Moored time-series sediment traps were employed at three different depths at the WCT-2 site (39°00'N, 147°00'E) in the western North Pacific from 19 November 1997 to 10 August 1999 (Table 1). The traps were set and recovered during the Western Pacific Environmental Assessment Study (WEST) CO_2 Ocean Sequestration for Mitigation of Climate Change (COSMIC) cruises in 1997, 1998, and 1999 aboard the R/V Daini Hakurei-maru (Mohiuddin et al., 2002). Sample cups at shallow and deep depths were replaced every 13 days from 19 November 1997 to 6 August 1998 and every 18 days from 26 August 1998 to 10 August 1999. The sample cups at middle depths were replaced every 22 days from 19 November 1997 to 10 August 1998 and every 30 days from 27 August 1998 to 10 August 1999. The cups were filled with 1% $HgCl_2$ seawater (pH = ~7). Recovered particles were separated into a coarse fraction (>1 mm diameter) and a fine fraction (<1 mm) by filtering. The coarse fraction was made up of scoriae and swimmers. The fine fraction was collected on a membrane filter (0.6 μm pore diameter), dried at 60°C for one day and milled using an agate mortar. Scoriae were picked with tweezers during grinding. The results of biogenic fluxes and foraminiferal associations at this station have been reported by Mohiuddin et al. (2002).

The multiple core CMC18, 30 cm long, was taken at 39°00.0'N, 146°56.0'E, at a depth of 5389 m during WEST COSMIC cruise NH99 of the R/V Daini Hakurei-maru on 7 August 1999. The sediments consist of dark olive brown diatomaceous silty clay

from 0 to 10 cm deep and olive black diatomaceous clay with ash patches from 10 to 30 cm deep (Fig. 3). The core was sampled every 0.31 cm, and 14 samples were selected for analysis.

The age model was created using the calendar ages converted from the AMS ^{14}C ages of six bulk organic matter samples (1380–8000 ^{14}C yrs. BP) using CALIB4.3 software and the marine98 calibration data set (Stuiver and Reimer, 1993) with a 400-year global reservoir correction (Table 2).

Analytical methods

Alkenones were analyzed by the modified method of Yamamoto et al. (2000b). Lipids were extracted from the fine fraction by five 5-min rounds of ultrasonication with 5 ml of dichloromethane-methanol (6:4), then concentrated and passed through a short bed of Na_2SO_4 to remove water. The lipid extract was separated into four fractions (F1: 3 ml of hexane; F2: 3 ml of hexane-toluene (3:1); F3: 4 ml of toluene; F4: 3 ml of toluene-methanol (3:1)) by column chromatography (SiO_2 with 5% distilled water; i.d., 5.5 mm; length, 45 mm). Then, *n*-$C_{36}H_{74}$ was added as an internal standard into the F3 (alkenones and alkenoates) fraction.

Gas chromatography of the F3 fraction was conducted using a Hewlett Packard 5890 series II gas chromatograph (GC) with on-column injection and electron pressure control systems and a flame ionization detector (FID). Samples were dissolved in hexane. Helium was used as a carrier gas, and the flow velocity was maintained at 30 cm/s. The column used was a Chrompack CP-Sil5CB (length, 60 m; i.d., 0.25 mm; thickness, 0.25 μm). The oven temperature was programmed from 70°C to 310°C at 20°C/min and then held at 310°C for 40 min. The standard deviations of the five

duplicate analyses averaged 0.008 for $U^{K'}_{37}$ (0.24°C) and 7.5% of the concentration for C_{37} alkenones.

Gas chromatography-mass spectrometry was conducted using a Hewlett Packard 5973 gas chromatograph-mass selective detector with on-column injection and electron pressure control systems and a quadrupole mass spectrometer. The GC column, oven temperature and carrier pressure programs were the same as described above. The mass spectrometer was run in the full-scan ion-monitoring mode (*m/z* 50–650). Electron impact spectra were obtained at 70 eV. Identification of compounds was achieved by comparison of their mass spectra and retention times with those of an extract from cultured *Emiliania huxleyi* (Yamamoto et al., 2000a) and those described in the literature (e.g., de Leeuw et al., 1980; Rechka and Maxwell, 1988).

The alkenone unsaturation index $U^{K'}_{37}$ was calculated from the concentrations of di- and tri-unsaturated C_{37} alken-2-ones using the following expression (Prahl et al., 1988):

$$U^{K'}_{37} = [C_{37:2}MK]/([C_{37:2}MK] + [C_{37:3}MK]).$$

Temperature was calculated according to the following equation based on an experimental result for the cultured strain 55a of *Emiliania huxleyi* (Prahl et al., 1988):

$$U^{K'}_{37} = 0.034T + 0.039,$$

where T = temperature [°C]); analytical accuracy was 0.24°C in our laboratory. Alkenone concentration is the total concentration of C_{37}–C_{39} alkenones. Alkenoate concentration is the total concentration of C_{37} methyalkenoates and C_{38} ethylalkenoate.

The F3 fraction was separated into four fractions (Ag-F1: 4 ml of dichloromethane; Ag-F2: 12 ml of dichloromethane (3:1); Ag-F3: 4 ml of diethyl ether; Ag-F4: 4 ml of methanol) by column chromatography (SiO_2 with 10% argentine nitrate; i.d., 5.5 mm; length, 45 mm). Alkadienones were eluted mostly in the Ag-F2 fraction.

Combined gas-chromatography-isotope ratio-mass spectrometry (GC/IRMS) for alkadienones was carried out using a Hewlett-Packard 5890 series II gas chromatograph with a capillary column coated with DB-5MS (60m length; i.d. 0.32 mm; 0.25 μm film thickness) combined with a Finnigan MAT delta S mass spectrometer through a combustion furnace at 840°C. The sample was dissolved in toluene and then injected into the on-column injection system. The oven temperature was programmed from 50°C to 280°C at 20°C/min. and from 280°C to 310°C at 5°C/min. and then maintained at 310°C for 35 min. As internal isotopic standards, *n*-$C_{37}H_{76}$, *n*-$C_{38}H_{78}$, and *n*-$C_{41}H_{84}$ were used. Data were converted to values relative to VPDB using standard delta notation. The analysis was repeated, and the average and standard deviation of the $\delta^{13}C$ values were calculated.

Organic carbon content was determined with a Yanaco MT-5 CHN analyzer after removal of carbonate by HCl vapor acidification in ceramic sample boats (Yamamuro and Kayanne, 1995). Carbonate content was calculated from the difference between total carbon and organic carbon contents. Opal content was analyzed using the sodium-carbonate leaching method modified from Mortlock and Froelich (1989) as described by Kawahata et al. (1998).

Calculation of mass accumulation rate in core CMC18

The accumulation rates of organic carbon (OCAR) and alkenones (Alkenone AR)

were calculated according to the following formulas:

$$\text{OCAR (mg/cm}^2\text{/kyr)} = \text{TOC (\%)} \times \text{DBD (g/cm}^3\text{)} \times \text{LSR (cm/kyr)} \times 10$$

$$\text{Alkenone AR (}\mu\text{g/cm}^2\text{/kyr)} = \text{Alkenones (}\mu\text{g/g-sed.)} \times \text{DBD (g/cm}^3\text{)} \times \text{LSR (cm/kyr)}$$

where AR is the accumulation rate, DBD is the dry bulk density, and LSR is the linear sedimentation rate. The DBD was obtained by the following regression equation between ten measured DBDs and depth (T. Fukuhara, unpublished data):

$$\text{DBD (g/cm}^3\text{)} = 0.00780 \times \text{Depth (cm)} + 0.324$$

3. Results

Sediment trap experiment

Two seasonal cycles were observed in both the compositions and the fluxes of biogenic matter and alkenones during the 21 months from November 1997 to August 1999. Fluxes of the total fine fraction, organic carbon, calcium carbonate and opal in the shallow and deep traps have been reported by Mohiuddin et al. (2002). Tables 3 and 4 present the fluxes of the above-mentioned biogenic materials in the middle trap and the fluxes of alkenones and alkenoates, respectively.

Opal content ranged from 28% to 63% with an average of 48%, implying that diatom frustules are a major component of the sinking particles at this site. The total fine fraction, organic carbon, calcium carbonate, and opal fluxes showed strong seasonal variability in traps at each depth (Fig. 4). In 1998, biogenic fluxes began to increase in early March and reached a maximum in late June/early July except for the

calcium carbonate flux in the shallow trap, which reached a maximum in early May, abruptly decreased in late July, and remained nearly constant after August. Traps at different depths showed similar variations. Fluxes increased gradually from November 1998 to January 1999 and increased more rapidly after February. The shallow trap showed double maxima, in March and May, while middle and deep traps showed a single maximum in early May. The biogenic fluxes in the middle and deep traps exceeded those in the shallow trap from April to June, which was attributed to the lateral influx of particles at deeper traps (Mohiuddin et al., 2002).

The alkenone concentration and flux also showed strong seasonal variability in traps at each depth (Figs. 5a and 5b). In 1998, the alkenone concentration and sinking flux increased abruptly in April, showed triple maxima, in mid-May, early July, and late October and decreased gradually after November to February 1999. In 1999, the alkenone concentration and sinking flux increased abruptly in mid-March and showed double maxima, in late April/early May and early July. Traps at the different depths showed similar variations except for the interval between April and May 1999, when the alkenone fluxes in the middle and deep traps exceeded those in the shallow trap. This phenomenon was consistent with the higher flux of total fine particles and biogenic materials at deeper traps during the same period (Fig. 4). The high alkenone flux from spring to fall reflects the repeated blooms of *Emiliania huxleyi* in this station (Y. Tanaka, per com.). Seasonal cycles in alkenone flux lagged behind those of the fluxes in total fine fraction and bulk biogenic components by about one month (Figs. 4 and 5b). The sinking particles were composed mainly of biogenic opal and calcium carbonate, implying that the total flux reflected mainly the sinking fluxes of diatom frustules and foraminifers. The time lag between bulk biogenic and alkenone fluxes is attributed to

the ecological succession of the blooming of alkenone-producing coccolithophores after the blooming of diatoms.

The $U^{K'}_{37}$–based temperature calculated using the culture calibration of Prahl et al. (1988) showed parallel changes at each depth, varying from 12°C to 24°C (Fig. 5). The temperatures calculated using the surface-water calibration of Conte et al. (2006) were generally higher than those by culture calibration, and the deviation was ~1°C in warm seasons and ~3°C in cold seasons. In this study, we used the culture calibration to obtain the $U^{K'}_{37}$–based temperature. The $U^{K'}_{37}$–based temperature decreased gradually by ~3°C from November 1997 to March 1998 during the low alkenone flux period, abruptly decreased in April at the beginning of the high alkenone flux period, was minimized (10–12°C) in May 1998, and then increased until September 1998 (Fig. 5c). The temperature decreased again after October 1998 to April 1999 and then increased after late April. This change was different from the SST change (Integrated Global Ocean Services System [IGOSS] weekly SST; Reynolds et al., 2002). The $U^{K'}_{37}$–based temperature was generally higher than the SST during the low alkenone flux period from fall to spring, while it was lower than the SST during the high alkenone flux period from spring to fall.

The $\delta^{13}C$ values of heptatriacontadien-2-one ($C_{37:2}$MK) and octatriacontadien-2-one and 3-one ($C_{38:2}$MK + $C_{38:2}$EK) ranged from -26.5‰ to -21.9‰ and from -25.2‰ to -21.9‰, respectively (Table 5; Fig. 6). The $\delta^{13}C$ values were nearly constant and higher than -24‰ from November 1997 to mid-March 1998. These values dropped once in early April, recovered in mid-April, were nearly constant until early May, and then decreased again from mid-May. They were generally constant during the low alkenone flux period, while they varied after the increase in alkenone flux in spring.

Core CMC18

Total organic carbon content (TOC) ranged from 0.66 to 1.51%, with an average of 0.91% (Table 6). The TOC decreased from the core top to ~4 cm deep (~2.3 ka) and gradually decreased downward below ~4 cm deep (~2.3 ka; Fig. 7a). The organic carbon accumulation rate (OCAR) ranged from 6.2 to 12.2 mg/cm^2/kyr with an exceptionally high peak interval between ~2.8 and ~6.6 cm deep (~2.2 ka and 2.4 ka; Fig. 7a). This high peak was due to the high linear sedimentation rate in this interval.

The alkenone concentration was highest at the core top, decreased abruptly downwards until 1.57 cm (~1.6 ka), and then increased with increasing depth (Fig. 7b). The decrease in alkenone concentration beneath the core top presumably resulted from diagenetic degradation. The alkenone AR showed a similar changing pattern with that of OCAR that showed a high peak interval from ~2.8 to ~6.6 cm deep (from ~2.2 ka to ~2.4 ka; Fig. 7b).

The $U^{K'}_{37}$–based temperature at the core top was 14.9°C, which is nearly identical to the mean annual SST at this site (15°C, Conkright et al., 2001). The $U^{K'}_{37}$–based temperature increased from ~9.7 ka to ~3.5 ka and decreased to 0.9 ka (Fig. 7c).

4. Discussion

Season and depth of alkenone production

The changes in $U^{K'}_{37}$–based temperature were different from those of the contemporary SST (Reynolds et al., 2002). The $U^{K'}_{37}$–based temperature was lower than the SST during the high alkenone flux period (spring to fall), while it was higher than the SST during the low alkenone flux period (fall to spring).

During periods of high alkenone flux, the $U^{K'}_{37}$–based temperatures were 0–7°C lower than the contemporary SSTs (Fig. 5c). This phenomenon has been previously reported for the northern Mediterranean Sea (Ternois et al., 1997), the central Arabian Sea (Prahl et al., 2000), the subtropical North Pacific (Prahl et al., 2005; Popp et al., 2006) and the subarctic NW Pacific (Harada et al., 2006) and has been attributed to either alkenone production at the thermocline depth (Ternois et al., 1997; Harada et al., 2006) or nutrient deficiency (Popp et al., 2006). Culture experiments have shown a decrease in $U^{K'}_{37}$ with nutrient deficiency (Epstein et al., 1998; Conte et al, 1998a; Yamamoto et al., 2000a). Such a physiological response is associated with the increase of the alkenoate/alkenone ratio (Conte et al., 1998a; Yamamoto et al., 2000a). In this study, the variation in the alkenoate/alkenone ratio did not correspond to the deviation of $U^{K'}_{37}$–based temperature from SST, suggesting that nutrient deficiency is less likely to explain the deviation. Genotypic variations in alkenone producers can also alter the $U^{K'}_{37}$ (Volkman et al., 1995; Sawada et al., 1996; Conte et al., 1998a; Yamamoto et al., 2000a). However, a coccolith study showed that *Emiliania huxleyi* always predominated with a minor contribution from *Gephyrocapsa oceanica* at this station (Y. Tanaka, unpublished data), although variations at the sub-species level were not investigated; there appears to be little seasonal variation in alkenone producers. This evidence suggests that subsurface production of alkenones is more likely to explain the deviation of $U^{K'}_{37}$–based temperature from SST rather than nutrient deficiency and genotypic variations. Because thermal stratification is developed after April in the western North Pacific (Fig. 2), the $U^{K'}_{37}$–based temperature most likely reflects the temperature at the thermocline. The depth profile of water temperature at the study site in the summer of 1998 indicates that the $U^{K'}_{37}$–based temperature corresponded to the temperature at ~30

m deep (Fig. 8). This correspondence suggests that the depth of alkenone production was ~30 m if there was no time lag between alkenone production and sinking. This estimated depth is 10 m shallower than that of the chlorophyll maximum (Fig. 8). If there was a time lag of maximum three months, the alkenone production depth must be shallower.

During periods of low alkenone flux, the $U^{K'}_{37}$–based temperatures were ~1–7°C higher than the contemporary SSTs. If the surface water calibration of Conte et al. (2006) is used, the deviation is more enhanced. Higher $U^{K'}_{37}$–based temperatures compared with contemporary SSTs in low alkenone flux periods have been previously reported from several regions such as the eastern North Pacific (Prahl et al., 1993), the Sargasso Sea (Conte et al., 1998b), the northwestern Mediterranean Sea (Sicre et al., 1999), the central Arabian Sea (Prahl et al., 2000), the subtropical North Pacific (Prahl et al., 2005; Popp et al., 2006) and the subarctic North Pacific (Harada et al., 2006). Conte et al. (1998b) and Sicre et al. (1999) attributed this phenomenon to the gradual sinking of alkenones that had been produced in the previous high alkenone flux period. Prahl et al. (2005) and Popp et al. (2006) suggested that the physiological response to light limitation in the deep chlorophyll maximum increased $U^{K'}_{37}$ during the winter flux maximum. However, no winter flux maximum was observed at our study site (Fig. 5), suggesting that the alkenone production was not significant in winter. Harada et al. (2006) proposed that alkenones produced in subtropical regions were transported into subarctic regions by the movement of meso-scale warm rings in the NW Pacific. We, however, also found higher $U^{K'}_{37}$–based temperatures compared with contemporary SSTs in low alkenone flux periods at site WCT-1 mooring sediment traps (25°N, 137°E) in the subtropical Pacific (M. Yamamoto, unpublished data). This finding suggests that

this phenomenon is not restricted in the subarctic region, but is common in the western North Pacific, being inconsistent with the hypothesis of Harada et al. (2006).

In this study, the $\delta^{13}C$ value of alkenones changed in small ranges during the low alkenone flux period (Fig. 6). Alkenones in haptophyte algae are more depleted in ^{13}C than inorganic carbon in seawater because of the preferential fixation of ^{12}C by photosynthetic enzymes (Jasper and Hayes, 1990). Culture studies have demonstrated that the fractionation of $\delta^{13}C$ between alkenones and inorganic carbon depends on the dissolved CO_2 concentration, growth rate, cellar surface area/volume ratio, and bicarbonate utilization (e.g., Laws et al., 1995, 1997; Bidigare et al., 1997; Popp et al., 1998). Thus the stable $\delta^{13}C$ value during the low alkenone flux period, along with the stable $U^{K'}_{37}$ value, suggests a common source of alkenones, which is consistent with the hypothesis of Conte et al. (1998b) and Sicre et al. (1999).

The gradual decrease in alkenone concentration from fall to spring suggests that the alkenones produced in early fall were suspended in the surface water during winter until sinking. When particle residence times are long enough, the lateral advection of allochthonous alkenones by strong surface currents can alter the alkenone signal (Rühlemann and Butzin, 2006; Conte et al., 2006). An ocean general circulation model study indicated that the average of surface current velocity was ~10 cm/sec (~8.6 km/day and ~260 km/month) during winters at site WCT-2 (Nonaka et al., 2006). The subsurface current velocity must be lower than the surface velocity. This low current velocity suggests that suspended alkenones could stay near the production area during winter, although it is also possible that the warm-water detrital alkenones were supplied by the Kuroshio in winters, if the residence time of detrital alkenones was long enough.

The following two questions, however, arise from this scenario. Why were the

suspended alkenones not degraded in the oxygenated surface water? What kind of process exports the suspended alkenones from the surface to deeper water? We speculate that the formation of organo-clay complex preserves alkenones in the surface water and also generates aggregates that can sink in the water column. Lithogenic matter makes up ~12–38% of total fine fraction (Shimamoto, unpublished data), and its flux ranged from 12 to 37 mg/m^2/d. The rate of deposition of mineral aerosol in this region is estimated to be ~27 mg/m^2/d, based on atmospheric observations (Duce et al., 1991). This correspondence suggests that that the contribution of eolian continental dust and volcanic ash (Olivarez et al., 1991) has constantly been significant at the study site. It is therefore likely that alkenones were protected from aerobic microbial degradation by incorporation into organo-clay complexes, and the aggregation of the organo-clay complex triggers the export from the surface water. This preservation-export process might be significant during periods of low alkenone flux, whilst the marine snow and fecal pellets dominate transport during periods of high alkenone flux.

Depth changes of biogenic and alkenone sinking fluxes

Biogenic and alkenone fluxes decreased exponentially with increasing depth (Figs. 9a and 9b). The biogenic fluxes were almost identical between the NH97 and NH98 intervals, while the alkenone flux in the NH97 interval was lower than that in the NH98 interval.

The relationship between sinking flux and depth is expressed by the following formulas:

$$F_Z = F_0 e^{-kZ}$$

where Z is depth (m), F_Z is the sinking flux at depth Z, F_0 is the presumed sinking flux at the sea surface, and k is the decomposition rate constant with depth. The half depth ($Z_{1/2}$) is calculated using the following equation:

$$Z_{1/2}\ (\mathrm{m}) = \ln 2/k = 0.693/k$$

Table 7 shows the calculated $Z_{1/2}$, F_0, and F_{5389} (the sinking flux at the sea bottom). The half depths of biogenic, alkenone and alkenoate fluxes in the NH97 interval were nearly equal to those in the NH98 interval. The half depths of opal, calcium carbonate, and organic carbon decreased in this descending order. The half depth of alkenones was much shallower than those of bulk biogenic components, implying that alkenones were more labile than bulk biogenic components.

The ratio of alkenone flux at shallow traps to that at deep traps showed strong seasonal variation (Fig. 10b). The ratio was higher in high alkenone flux periods (spring to fall) than in low alkenone flux periods (fall to spring). This tendency implies either that the sinking rate was higher or that sinking particles were more stable during low alkenone flux periods. Sinking particles tend to be larger during blooming in general, which is inconsistent with faster sinking during low alkenone flux periods, suggesting that sinking particles were more stable during low alkenone flux periods. This implies that fresh and labile particles sink during high alkenone flux periods, while old and stable particles sink during low alkenone flux periods.

The half depth of alkenoates was much deeper than that of alkenones and was at the same level as the bulk biogenic components (Table 7). The abundance ratio of

alkenoates to alkenones consistently increased with increasing depth (Fig. 9c). This trend implies that alkenoates are more stable than alkenones, which is consistent with the conclusion of Prahl et al. (1993).

The abundance ratios of alkenoates to alkenones in late 1998 and 1999 were higher than those in previous periods (Fig. 10a). Conte et al. (1998a) and Yamamoto et al. (2000a) reported an increase in the ethylalkenoate/alkenone ratio with nutrient deficiencies in cultured strains of *Emiliania huxleyi* and *Gephyrocapsa oceanica*. Goes et al. (2001) found that the estimated nitrate concentration in March 1998 was higher than that in March 1999 in the Kuroshio–Oyashio transition because of the El Niño influence in 1998. The nutrient supply in this region is driven by the winter mixing of the ocean surface water, which is closely related to the Aleutian Low (Goes et al., 2001). The Aleutian Low is enhanced in El Niño conditions by the excitation of the Pacific–North America teleconnection pattern (Wallace and Gutzler, 1981). These results suggest that the high alkenoate/alkenone ratio in 1998 may have reflected the physiological response of alkenone producers to nutrient enrichment, which was presumably related to the El Niño.

A comparison of organic carbon flux at the bottom of the water column with the core-top OCAR of Core CMC18 provides the preservation efficiency of organic carbon at the water-sediment interface. The organic carbon flux at the bottom of the water column estimated by the sediment trap was 3.5 and 4.3 mg/m^2/d during the NH97 and NH98 sampling intervals, respectively (Table 7). The NH97 interval did not cover an entire year and did not include the autumn high flux season; thus the organic carbon flux was underestimated. The NH98 interval covered an entire year but also included periods of significant lateral influx into deeper traps; thus the organic carbon flux was

overestimated. Because the core-top OCAR of Core CMC18 was 8.7 mg/cm^2/kyr (0.24 mg/m^2/d; Table 6), the preservation efficiency of organic carbon is estimated to be ~5.5–6.7%.

In the same way, the preservation efficiency of alkenones can be obtained. Fluxes of alkenone sinking to the bottom of the water column were estimated by the sediment trap experiment as 0.79 and 1.54 μg/m^2/d for the NH97 and NH98 sampling intervals, respectively (Table 7). Because the core-top alkenone AR was 1.50 μg/cm^2/kyr (0.041 μg/m^2/d; Table 6), the preservation efficiency of alkenones is estimated to be ~2.7–5.2%.

Changes in the alkenone unsaturation index through water and sediment columns

The flux-weighted average $U^{K'}_{37}$–based temperature (integrated production temperature, IPT; defined by Conte et al., 1992) showed complex trends with depth (Fig. 9d). The IPT constantly increased with increasing depth in the NH97 sampling interval, while it increased slightly from shallow to middle traps and decreased to the deep trap in the NH98 sampling interval. The $U^{K'}_{37}$–based temperature in the shallow trap was always lower than that in the deep traps in the NH97 interval, while this was not the case in the NH98 interval (Fig. 5c). The temperature at shallow traps was often higher from September to December 1998 and April to July 1999 (Fig. 10c). The lower $U^{K'}_{37}$–based temperature at the deep trap in these periods resulted in the decreasing trend of IPT in the NH98 interval.

The downward increase in $U^{K'}_{37}$–based temperature observed in most periods suggests that the $U^{K'}_{37}$ is affected by alterations in the water column and to the preferential degradation or dissolution of tri-unsaturated alkenone relative to

di-unsaturated alkenone. Although most studies showed that the degradation of alkenones does not change $U^{K'}_{37}$ (e.g., Bentaleb et al., 1999; Sicre et al., 1999; Grimalt et al., 2000), Freeman and Wakeham (1992) argued that the degradation of alkenones increases $U^{K'}_{37}$ in the water column. With regard to the lower $U^{K'}_{37}$–based temperature at deep traps, the larger total fine flux in deeper traps in some intervals during these periods suggests the possibility of a lateral influx of alkenones produced in cooler waters to deeper traps.

The IPT at the deep trap was 14.5°C in the NH98 interval, which is 0.4°C lower than the $U^{K'}_{37}$–based temperature at the core top (14.9°C). This difference of estimated temperatures between deep-trap and core-top sediment ranged within the error of alkenone paleothermometry (Prahl et al., 1988). This result indicates that the degradation at the water-sediment interface did not affect the $U^{K'}_{37}$, an observation that is consistent with previous observations (Prahl et al., 1993; 2001; Müller and Fischer, 2001).

Acknowledgments: We thank Kazuko Hino and Etsuko Kamata (Geological Survey of Japan) and Noriko Edasawa (Hokkaido University) for analytical assistance in the laboratory. Special thanks are due to the members of NEDO WEST-COSMIC “Carbon Dioxide Ocean Sequestration for Mitigation of Climate Change” and the staff of the General Environmental Technos Co. LTD. for sampling and their helpful discussions, to Tomohisa Irino, Ken Sawada and Youichi Tanimoto (HU) for their valuable suggestions, and to Masatoshi Komiya (GSJ) for his help in analysis. We also acknowledge three anonymous reviewers for improving the manuscript. This study was financially supported by the New Energy and Industrial Technology Development Organization

(NEDO) the Agency of Industrial Science and Technology.

References:

Bentaleb, I., Grimalt, J.O., Vidussi, F., Marty, J.-C., Martin, V., Denis, M., Hatte, C., Fontugne, M., 1999. The C_{37} alkenone record of seawater temperature during seasonal thermocline stratification. Marine Chemistry 64, 301-313.

Bidigare, R.R., Fluegge, A., Freeman, K.H., Hanson, K.L., Hayes, J.M., Hollander, D., Jasper, J.P., King, L.L., Laws, E.A., Milder, J.S.G., Millero, F.J., Pancost, R., Popp, B.N., Steinberg, P.A., Wakeham, S.G., 1997. Consistent fractionation of ^{13}C in nature and in the laboratory: growth-rate effects in some haptophyte algae. Global Biogeochemical Cycles 11, 279-292.

Brassell, S.C., Eglinton, G., Marlowe, I.T., Pflaumann, U., Sarnthein, M., 1986. Molecular stratigraphy: a new tool for climatic assessment. Nature 320, 129-133.

Brassell, S. C., 1993. Applications of biomarkers for delineating marine paleoclimatic fluctuations during the Pleistocene. In Engel, M.H., Macko, S.A. (Eds.), Organic Geochemistry, Chapter 34, Plenum Press, New York, pp. 699-738.

Conte, M.H., Eglinton, G., Madureira, L.A.S., 1992. Long-chain alkenones and alkyl alkenoates as palaeotemperature indicators: their production, flux and early sedimentary diagenesis in the Eastern North Atlantic. Organic Geochemistry 19, 287-298.

Conte, M.H., Thompson, A., Lesley, D., Harris, R.P., 1998a. Genetic and physiological influences on the alkenone/alkenoate versus growth temperature relationship in *Emiliania huxleyi* and *Gephyrocapsa oceanica*. Geochimica et Cosmochimica Acta 62, 51-68.

Conte, M.H., Weber, J.C., Ralph, N., 1998b. Episodic particle flux in the deep Sargasso Sea: an organic geochemical assessment. Deep-Sea Research I 45, 1819-1841.

Conte, M. H., Sicre, M.-A., Rühlemann, C., Weber, J. C., Schulte, S., Schulz-Bull, D., Blanz, T., 2006. Global temperature calibration of the alkenone unsaturation index ($U^{K'}_{37}$) in surface waters and comparison with surface sediments. Geochemistry Geophysics Geosystems, 7, Q02005, doi:10.1029/2005GC001054.

Conkright, M.E., et al. 2002. World Ocean Atlas 2001: Objective Analyses, Data Statistics, and Figures, CD-ROM Documentation. National Oceanographic Data Center, Silver Spring, MD, 17 pp.

Duce, R. A., Liss, P. S., Merrill, J. T., Atlas, E. L., Buat-Menard, P., Hicks, B. B., Miller, J. M., Prospero, J. M., Arimoto, R., Church, T. M., Ellis, W., Galloway, J. N., Hansen, L., Jickells, T. D., Knap, A. H., Reinhardt, K. H., Schneider, B., Soudine, A., Tokos, J. J., Tsunogai, S., Wollast, R., Zhou, M., 1991. The atmospheric input of trace species to the world ocean. Global Biogeochem. Cycles 5, 193-259, doi:10.1029/91GB01778.

Epstein, B.L., D'Hondt, S., Quinn, J.G., Zhang, J. and Hargraves, P.E., 1998. An effect of dissolved nutrient concentrations on alkenone-based temperature estimates. Paleoceanography 13, 122-126.

Freeman, K.H., Wakeham, S.G., 1992. Variations in the distributions and isotopic compositions of alkenones in Black Sea particles and sediments. Organic Geochemistry 19, 277-285.

Goes, J.I., Gomes, H.R., Limsakul, A., Balch, W.M., Saino, T., 2001. El Niño related interannual variations in biological production in the North Pacific as evidenced by satellite and ship data. Progress in Oceanography 49, 211-225.

Gong, C., Hollander, D.J., 1999. Evidence for differential degradation of alkenones under contrasting bottom water oxygen conditions: Implication for paleotemperature reconstruction. Geochimica et Cosmochimica Acta 63, 405-411.

Grimalt, J. O., Rullkötter, J., Sicre, M.-A., Summons, R., Farrington, J., Harvey, H. R., Goni, M., Sawada, K., 2000. Modifications of the C_{37} alkenone and akenoate composition in the water column and sediment: Possible implications for sea surface temperature estimates in paleoceanography. Geochemistry Geophysics Geosystems 1, 2000GC000053.

Harada, N., Sato, M., Shiraishi, A., Honda, M.C., 2006. Characteristics of alkenone distributions in suspended and sinking particles in the northwestern North Pacific. Geochimica et Cosmochimica Acta, 70, 2045-2062.

Hoefs, M.J.L., Versteegh, G.J.M., Rijpstra, W.I.C., de Leeuw, J.W., Sinninghe Damsté, J.S., 1998. Post-depositional oxic degradation of alkenones: Implications for the measurement of paleo sea surface temperatures. Paleoceanography 13, 42-49.

Jasper, J.P., Hayes, J.M., 1990. A carbon isotope record of CO_2 levels during the late Quaternary. Nature 347, 462-464.

Kawahata, H., Yamamuro, M., Ohta, H., 1998. Seasonal and vertical variations of sinking particle fluxes in the western Caroline Basin. Oceanologica Acta, 21, 521-532.

Laws, E.A., Popp, B.N., Bidigare, R.R., Kennicutt, M.C. and Macko, S.A., 1995. Dependence of phytoplankton carbon isotopic composition on growth rate and $[CO_2]_{aq}$: Theoretical considerations and experimental results. Geochimica et Cosmochimica Acta 59, 1131-1138.

Laws, E.A., Bidigare, R.R., Popp, B.N., 1997. Effect of growth rate and CO_2

concentration on carbon isotopic fractionation by the marine diatom *Phaeodactylum tricornutum*. Limnology and Oceanography 42, 1552-1560.

de Leeuw, J.W., van der Meer, F.W., Rijpstra, W.I.C., Schenck, P.A., 1980. On the occurrence and structural identification of long chain unsaturated ketones and hydrocarbons in sediments. In Douglas, A.G., Maxwell, J.R. (Eds.), Advances in Organic Geochemistry 1979, Pergamon Press, Oxford, pp. 211-217.

Marlowe, I.T., Brassell, S.C., Eglinton, G. and Green, J.C., 1984. Long chain unsaturated ketones and esters in living algae and marine sediments. Organic Geochemistry 6, 135-141.

Marlowe, I.T., Brassell, S.C., Eglinton, G., Green, J.C., 1990. Long-chain alkenones and alkyl alkenoates and the fossil coccolith record of marine sediments. Chemical Geology 88, 349-375.

Mohiuddin, M.M., Nishimura, A., Tanaka, Y., Shimamoto, A., 2002. Regional and interannual productivity of biogenic components and planktonic foraminiferal fluxes in the northwestern Pacific Basin. Marine Micropaleontology 45, 57-82.

Mortlock, R.A., Froelich, P.N., 1989. A simple method for the rapid determination of biogenic opal in pelagic marine sediments. Deep-Sea Research 36, 1415-1426.

Müller, P.J., Kirst, G., Ruhland, G., von Storch, I., Rosell-Melé, A., 1998. Calibration of the alkenone paleotemperature index $U^{K'}_{37}$ based on core tops from the eastern South Atlantic and the global ocean (60°N-60°S). Geochimica et Cosmochimica Acta 62, 1757-1722.

Müller, P.J., Fischer, G., 2001. A 4-year sediment trap record of alkenones from the filamentous upwelling region off Cape Blanc, NW Africa and a comparison with distributions in underlying sediments. Deep-Sea Research I 48, 1877-1903.

Nonaka, M., Kawamura, H., Tanimoto, Y., Kagimoto, T, Sasaki, H., 2006. Decadal variability in the Kuroshio-Oyashio Extension simulated in an eddy-resolving OGCM. Journal of Climate 19, 1970-1989.

Ohkouchi, N., Kawamura, K., Kawahata, H., Okada, H., 1999. Depth range of alkenone production in the central Pacific Ocean. Global Biogeochemical Cycles 13, 2, 695-704.

Olivarez, A. M., Owen, R. M., Rea, D. K., 1991. Geochemistry of eolian dust in Pacific pelagic sediments: Implications for paleoclimatic interpretations. Geochimica et Cosmochimica Acta 55, 2147-2158.

Popp, B.N., Laws, E.A., Bidigare, R.R., Gore, J.E., Hanson, K.L., Wakeham, S.G., 1998. Effect of phytoplankton cell geometry on carbon isotopic fractionation. Geochimica et Cosmochimica Acta 62, 69-77.

Popp, B.N., Prahl, F.G., Wallsgrove, R.J., Tanimoto, J., 2006. Seasonal patterns of alkenone production in the subtropical oligotrophic North Pacific. Paleoceanogeaphy 21, PA1004, doi:10.1029/2005PA001165.

Prahl, F.G., Wakeham, S.G., 1987. Calibration of unsaturation patterns in long-chain ketone compositions for palaeotemperature assessment. Nature 330, 367-369.

Prahl, F.G., Muehlhausen, L.A., Zahnle, D.L., 1988. Further evaluation of long-chain alkenones as indicators of paleoceanographic conditions. Geochimica et Cosmochimica Acta 52, 2303-2310.

Prahl, F.G., Collier, R.B., Dymond, J., Lyle, M., Sparrow, M.A., 1993. A biomarker perspective on prymnesiophyte productivity in the northeast Pacific Ocean. Deep-Sea Research I 40, 2061-2076.

Prahl, F. G., Dymond, J, Sparrow, M. A., 2000. Annual biomarker record for export

production in the central Arabian Sea. Deep-Sea Research II 47, 1581-1604.

Prahl, F.G., Pilskaln, C.H., Sparrow, M.A., 2001. Seasonal record for alkenones in sedimentary particles from the Gulf of Maine. Deep-Sea Research I 48, 515-528.

Prahl, F.G., Popp. B.N., Karl, D.M., Sparrow, M.A., 2005. Ecology and biogeochemistry of alkenone production at Station ALOHA. Deep-Sea Research I 52, 699-719. doi: 10.1016/j.dsr.2004.12.001.

Rechka, J.A., Maxwell, J.R., 1988. Characterisation of alkenone temperature indicators in sediments and organisms. Organic Geochemistry 13, 727-734.

Reynolds, R.W., Rayner, N.A., Smith, T.M., Stokes, D.C., Wang, W., 2002. An improved in situ and satellite SST analysis for climate. Journal of Climate 15, 1609-1625.

Rühlemann, C., Butzin, M., 2006. Alkenone temperature anomalies in the Brazil-Malvinas Confluence area caused by lateral advection of suspended particulate material. Geochemistry Geophysics Geosystems, 7, Q10015, doi:10.1029/2006GC001251.

Sawada, K., Handa, N., Shiraiwa, Y., Danbara, A., Montani, S., 1996. Long-chain alkenones and alkyl alkenoates in the coastal and pelagic sediments of the northwest North Pacific, with special reference to the reconstruction of *Emiliania huxleyi* and *Gephyrocapsa oceanica* ratios. Organic Geochemistry 24, 751-764.

Sawada, K., Handa, N., Nakatsuka, T., 1998. Production and transport of long-chain alkenones and alkyl alkenoates in sea water column in the northwestern Pacific off central Japan. Marine Chemistry 59, 219-234.

Sicre, M.-A., Ternois, Y., Miquel, J.-C., Marty, J.-C., 1999. Alkenones in the northwestern Mediterranean sea: interannual variability and vertical transfer.

Geophysical Research Letters 26, 1735-1738.

Sicre, M.-A., Labeyrie, L., Ezat, U., Duprat, J., Turon, J. L., Schimidt, S., Michel, E., Mazaud, A., 2005. Mid-latitude Southern Indian Ocean response to Northern Hemisphere Heinrich events. Earth and Planetary Science Letters, 240, 724-731.

Stuiver, M., Reimer, P., 1993. Extended ^{14}C database and revised CALIB 3.0 ^{14}C age model calibration program. Radiocarbon 35, 215-230.

Ternois, Y., Sicre, M.-A., Boireau, A., Conte, M.H., Eglinton, G., 1997. Evaluation of long-chain alkenones as paleo-temperature indicators in the Mediterranean Sea. Deep-Sea Research I 44, 271-286.

Volkman, J.K., Eglinton, G., Corner, E.D.S., Sargent, J.R., 1980. Novel unsaturated straight-chain C_{37}-C_{39} methyl and ethyl ketones in marine sediments and a coccolithophore *Emiliania huxleyi*. In Douglas, A.G., Maxwell, J.R. (Eds.), Advances in Organic Geochemistry 1979, Pergamon Press, Oxford, pp. 219-227.

Volkman, J.K., Barrett, S.M., Blackburn, S.I., Sikes, E.L., 1995. Alkenones in *Gephyrocapsa oceanica*: Implications for studies of paleoclimate. Geochimica et Cosmochimica Acta 59, 513-520.

Wallace, J.M., Gutzler, D.S., 1981. Teleconnections in the geopotential hight field during the Northern Hemisphere winter. Monthly Weather Reviews, 109, 784-812.

Yamamoto, M., Shiraiwa, Y., Inouye, I., 2000a. Physiological responses of lipids in *Emiliania Huxleyi* and *Gephyrocapsa oceanica* (Haptophyceae) to growth status and their implications for alkenone paleothermometry. Organic Geochemistry 31, 799-811.

Yamamoto, M., Yamamuro, M., Tada, R., 2000b. Late Quaternary records of organic carbon, calcium carbonate and biomarkers from Site 1016 off Point Conception,

California margin. Proceedings of Ocean Drilling Program Scientific Results 167, 183-194.

Yamamuro, M., Kayanne, H., 1995. Rapid direct determination of organic carbon and nitrogen in carbonate bearing sediments using Yanaco MT-5 CHN analyzer. Limnology and Oceanography 39, 1726-1733.

Table Captions:

Table 1 Location, sampling periods and trap depths of the WCT-2 mooring sediment trap system

Table 2 The ^{14}C ages of bulk organic matter from core CMC18 at 39°00'N, 146°56'E

Table 3 Contents and sinking fluxes of biogenic components in the middle trap from November 1997 to August 1999 at site WCT-2

Table 4 Concentrations and sinking fluxes of alkenones and alkenoates and $U^{K'}_{37}$ from November 1997 to August 1999 at site WCT-2

Table 5 Carbon isotopic compositions of heptatriacontadien-2-one ($C_{37:2}$MK) and the mixture of octatriacontadien-2-one and octatriacontadien-3-one ($C_{38:2}$MK & EK) collected in the shallow trap from November 1997 to August 1998 at site WCT-2.

Table 6 Concentrations and accumulation rates of organic carbon, alkenones and

alkenoates and $U^{K'}_{37}$ in core CMC18 at 39°00'N, 146°56'E

Table 7 Sinking fluxes of total fine particles, biogenic materials, alkenones and alkenoates and integrated production temperatures at site WCT-2

Figure Captions:

Fig. 1 Map showing the location of the study site (WCT-2).

Fig. 2 (a) Monthly mean temperatures at various depths. (b) The depth profiles of temperature in different seasons at the WCT-2 site (39°N, 147°E).

Fig. 3 Lithology of multiple-core CMC18 at 39°00'N, 146°56'E.

Fig. 4 Changes in the sinking fluxes of (a) the total fine fraction of less than 1-mm diameter, (b) organic carbon (OC), (c) calcium carbonate ($CaCO_3$) and (d) opal from November 1997 to August 1999 at site WCT-2. Data for shallow and deep traps are from Mohiuddin et al. (2002).

Fig. 5 Changes in (a) the concentration and (b) sinking flux of alkenones and (c) $U^{K'}_{37}$–based temperature from November 1997 to August 1999. The IGOSS weekly SSTs at 39°N, 147°E are from Reynolds et al. (2002).

Fig. 6 Changes in the $\delta^{13}C$ of heptatriacontadien-2-one ($C_{37:2}$MK) and

octatriacontadien-2-one and 3-one ($C_{38:2}$MK&EK) and the alkenone sinking flux in the shallow trap from November 1997 to August 1998.

Fig. 7 (a) Total organic carbon contents (TOC) and accumulation rates (OCAR), (b) alkenone concentrations and accumulation rates and (c) $U^{K'}_{37}$–based temperatures in core CMC18.

Fig. 8 Depth profiles of the measured temperature and chlorophyll a concentration (Chl. a) when the trap was recovered on 26 August 1998. The $U^{K'}_{37}$–based temperature of the cup from 24 July to 6 August 1998 and the expected production depth (EPD) are also presented.

Fig. 9 Depth changes in the (a) biogenic fluxes, (b) alkenone flux, (c) alkenoate/alkenone ratio and (d) flux-weighted average $U^{K'}_{37}$–based temperature (IPT defined by Conte et al., 1992).

Fig. 10 Changes in (a) the ratio of alkenoates to alkenones, (b) the ratio of alkenone flux in the shallow traps to that in deep traps, and (c) the difference of $U^{K'}_{37}$–based temperature between shallow and deep traps from November 1997 to August 1999.

Table 1

Location			Seafloor depth (m)	Duration	Trap depth (m)		
					Shallow	Middle	Deep
39	00.09'N, 146	59.66'E	5356	19 November 1997 to 6 August 1998	1366	3056	4786
39	01.00'N, 147	00.06'E	5322	27 August 1998 to 10 August 1999	1332	2472	4752

Table 2

Depth (cm)	Conventional age (yr.BP)	1σ	Calendar age (Cal. yr. BP)
0.6	1380	40	887
2.5	2500	40	2142
4.1	2590	40	2293
7.9	2760	40	2460
12.3	3710	40	3625
21.7	8000	50	8421

Table 3

Name	Depth	Sampling period		Content % in total fine fraction			Sinking flux (mg/m²/d)			
	m	Open	Close	OC	$CaCO_3$	Opal	Fine fraction	OC	$CaCO_3$	Opal
Middle trap										
NH97 sampling interval										
39N,A-01	3056	19-Nov-97	11-Dec-97	4.55	27.82	42.44	88.57	4.03	24.64	37.59
39N,A-02	3056	11-Dec-97	2-Jan-98	4.88	27.08	45.29	57.22	2.79	15.49	25.91
39N,A-03	3056	2-Jan-98	24-Jan-98	4.85	19.84	50.19	80.68	3.91	16.01	40.50
39N,A-04	3056	24-Jan-98	15-Feb-98	4.20	21.87	43.60	91.41	3.84	20.00	39.86
39N,A-05	3056	15-Feb-98	9-Mar-98	4.09	19.01	52.66	86.38	3.53	16.42	45.49
39N,A-06	3056	9-Mar-98	31-Mar-98	4.02	18.40	48.76	147.59	5.93	27.16	71.96
39N,A-07	3056	31-Mar-98	22-Apr-98	3.81	19.23	49.64	161.30	6.15	31.02	80.07
39N,A-08	3056	22-Apr-98	14-May-98	3.84	24.71	48.94	152.85	5.87	37.77	74.80
39N,A-09	3056	14-May-98	5-Jun-98	3.42	24.67	51.52	165.29	5.65	40.77	85.15
39N,A-10	3056	5-Jun-98	27-Jun-98	3.58	26.26	49.89	162.43	5.81	42.65	81.03
39N,A-11	3056	27-Jun-98	19-Jul-98	4.27	14.32	51.62	187.71	8.02	26.88	96.89
39N,A-12	3056	19-Jul-98	10-Aug-98	4.74	17.34	49.39	62.10	2.94	10.77	30.67
NH98 sampling interval										
39N,A-01	2472	27-Aug-98	14-Sep-98	5.49	18.20	40.76	129.24	7.10	23.52	52.68
39N,A-02	2472	14-Sep-98	14-Oct-98	5.26	19.21	40.91	113.69	5.98	21.84	46.52
39N,A-03	2472	14-Oct-98	13-Nov-98	5.51	24.52	39.18	118.66	6.54	29.10	46.49
39N,A-04	2472	13-Nov-98	13-Dec-98	4.91	24.36	38.22	110.81	5.44	26.99	42.35
39N,A-05	2472	13-Dec-98	12-Jan-99	4.11	20.00	44.89	171.09	7.03	34.22	76.81
39N,A-06	2472	12-Jan-99	11-Feb-99	3.52	16.13	44.07	186.95	6.58	30.16	82.38
39N,A-07	2472	11-Feb-99	13-Mar-99	3.15	13.59	49.44	269.68	8.49	36.65	133.34
39N,A-08	2472	13-Mar-99	12-Apr-99	3.20	12.79	54.39	274.69	8.79	35.14	149.41
39N,A-09	2472	12-Apr-99	12-May-99	2.95	9.01	56.74	558.69	16.48	50.32	316.98
39N,A-10	2472	12-May-99	11-Jun-99	2.93	16.11	52.11	311.16	9.12	50.12	162.13
39N,A-11	2472	11-Jun-99	11-Jul-99	3.98	29.08	40.92	173.87	6.92	50.56	71.15
39N,A-12	2472	11-Jul-99	10-Aug-99	4.06	17.92	43.02	89.88	3.65	16.11	38.67

OC = organic carbon

Table 4

Name	Depth m	Sampling period Open	Close	Alkenones µg/g-bulk sample	Alkenoates µg/g	Alkenones µg/m²/d	U^{K}_{37}'
Shallow trap							
NH97 sampling interval							
39N,U-01	1366	19-Nov-97	2-Dec-97	52.21	0.66	1.13	0.69
39N,U-02	1366	2-Dec-97	15-Dec-97	38.36	0.34	4.32	0.68
39N,U-03	1366	15-Dec-97	28-Dec-97	38.09	0.24	2.00	0.59
39N,U-04	1366	28-Dec-97	10-Jan-98	23.13	0.25	1.78	0.59
39N,U-05	1366	10-Jan-98	23-Jan-98	19.11	0.08	0.75	0.61
39N,U-06	1366	23-Jan-98	5-Feb-98	20.36	0.12	1.30	0.60
39N,U-07	1366	5-Feb-98	18-Feb-98	14.40	0.09	1.57	0.60
39N,U-08	1366	18-Feb-98	3-Mar-98	13.32	0.19	1.38	0.58
39N,U-09	1366	3-Mar-98	16-Mar-98	10.41	0.19	1.99	0.58
39N,U-10	1366	16-Mar-98	29-Mar-98	8.41	0.12	1.49	0.62
39N,U-11	1366	29-Mar-98	11-Apr-98	7.73	0.11	1.68	0.59
39N,U-12	1366	11-Apr-98	24-Apr-98	9.84	0.19	2.18	0.59
39N,U-13	1366	24-Apr-98	7-May-98	27.60	0.46	7.98	0.47
39N,U-14	1366	7-May-98	20-May-98	41.83	0.42	11.84	0.46
39N,U-15	1366	20-May-98	2-Jun-98	44.81	0.64	10.43	0.45
39N,U-16	1366	2-Jun-98	15-Jun-98	19.78	0.26	5.73	0.53
39N,U-17	1366	15-Jun-98	28-Jun-98	18.16	0.21	5.09	0.52
39N,U-18	1366	28-Jun-98	11-Jul-98	66.88	0.56	29.51	0.52
39N,U-19	1366	11-Jul-98	24-Jul-98	NA	NA	NA	NA
39N,U-20	1366	24-Jul-98	6-Aug-98	44.84	0.00	6.93	0.56
NH98 sampling interval							
39N,U-01	1332	27-Aug-98	2-Sep-98	NA	NA	NA	NA
39N,U-02	1332	2-Sep-98	20-Sep-98	62.38	1.38	8.83	0.61
39N,U-03	1332	20-Sep-98	8-Oct-98	63.97	1.08	5.39	0.76
39N,U-04	1332	8-Oct-98	26-Oct-98	88.51	1.29	7.83	0.71
39N,U-05	1332	26-Oct-98	13-Nov-98	40.41	1.15	4.53	0.70
39N,U-06	1332	13-Nov-98	1-Dec-98	33.86	1.32	3.15	0.71
39N,U-07	1332	1-Dec-98	19-Dec-98	30.68	1.91	3.73	0.66
39N,U-08	1332	19-Dec-98	6-Jan-99	13.32	0.40	2.42	0.67
39N,U-09	1332	6-Jan-99	24-Jan-99	11.28	0.31	2.06	0.63
39N,U-10	1332	24-Jan-99	11-Feb-99	7.43	0.60	1.32	0.60
39N,U-11	1332	11-Feb-99	1-Mar-99	4.12	0.20	1.49	0.61
39N,U-12	1332	1-Mar-99	19-Mar-99	4.30	0.27	1.83	0.55
39N,U-13	1332	19-Mar-99	6-Apr-99	26.31	0.64	7.34	0.51
39N,U-14	1332	6-Apr-99	24-Apr-99	29.22	0.54	6.63	0.39
39N,U-15	1332	24-Apr-99	12-May-99	51.79	1.13	13.99	0.45
39N,U-16	1332	12-May-99	30-May-99	26.78	1.24	8.56	0.47
39N,U-17	1332	30-May-99	17-Jun-99	39.56	1.55	6.63	0.53
39N,U-18	1332	17-Jun-99	5-Jul-99	102.87	3.27	20.88	0.51
39N,U-19	1332	5-Jul-99	23-Jul-99	76.98	1.05	11.65	0.58
39N,U-20	1332	23-Jul-99	10-Aug-99	NA	NA	NA	NA
Middle trap							
NH97 sampling interval							
39N,A-01	3056	19-Nov-97	11-Dec-97	38.43	1.08	3.43	0.64
39N,A-02	3056	11-Dec-97	2-Jan-98	19.62	0.39	1.14	0.65
39N,A-03	3056	2-Jan-98	24-Jan-98	16.42	0.15	1.34	0.61
39N,A-04	3056	24-Jan-98	15-Feb-98	11.51	0.31	1.06	0.66
39N,A-05	3056	15-Feb-98	9-Mar-98	10.62	0.25	0.92	0.62
39N,A-06	3056	9-Mar-98	31-Mar-98	6.78	0.16	1.02	0.64
39N,A-07	3056	31-Mar-98	22-Apr-98	7.90	0.09	1.30	0.59
39N,A-08	3056	22-Apr-98	14-May-98	10.31	0.12	1.58	0.54
39N,A-09	3056	14-May-98	5-Jun-98	17.67	0.75	2.94	0.47
39N,A-10	3056	5-Jun-98	27-Jun-98	9.90	0.16	1.62	0.52
39N,A-11	3056	27-Jun-98	19-Jul-98	19.69	0.38	3.72	0.53
39N,A-12	3056	19-Jul-98	10-Aug-98	24.27	0.25	1.55	0.60
NH98 sampling interval							
39N,A-01	2472	27-Aug-98	14-Sep-98	25.61	0.35	3.31	0.63
39N,A-02	2472	14-Sep-98	14-Oct-98	24.23	0.39	2.76	0.69
39N,A-03	2472	14-Oct-98	13-Nov-98	33.84	0.76	4.02	0.84
39N,A-04	2472	13-Nov-98	13-Dec-98	23.68	1.00	2.62	0.68
39N,A-05	2472	13-Dec-98	12-Jan-99	15.39	0.77	2.63	0.65
39N,A-06	2472	12-Jan-99	11-Feb-99	6.99	0.46	1.31	0.65
39N,A-07	2472	11-Feb-99	13-Mar-99	4.85	0.46	1.31	0.63
39N,A-08	2472	13-Mar-99	12-Apr-99	7.14	0.34	1.96	0.53
39N,A-09	2472	12-Apr-99	12-May-99	25.29	0.76	14.13	0.44
39N,A-10	2472	12-May-99	11-Jun-99	15.75	1.17	4.90	0.48
39N,A-11	2472	11-Jun-99	11-Jul-99	47.70	1.20	8.29	0.54
39N,A-12	2472	11-Jul-99	10-Aug-99	22.56	2.46	2.03	0.61

Table 4 continue

Deep trap							
NH97 sampling interval							
39N,L-01	4786	19-Nov-97	2-Dec-97	NA	NA	NA	NA
39N,L-02	4786	2-Dec-97	15-Dec-97	18.81	0.37	1.97	0.70
39N,L-03	4786	15-Dec-97	28-Dec-97	NA	NA	NA	NA
39N,L-04	4786	28-Dec-97	10-Jan-98	14.84	0.39	1.41	0.63
39N,L-05	4786	10-Jan-98	23-Jan-98	10.61	0.32	0.99	0.64
39N,L-06	4786	23-Jan-98	5-Feb-98	8.42	0.23	1.14	0.70
39N,L-07	4786	5-Feb-98	18-Feb-98	9.35	0.28	0.67	0.64
39N,L-08	4786	18-Feb-98	3-Mar-98	8.26	0.55	0.55	0.60
39N,L-09	4786	3-Mar-98	16-Mar-98	6.91	0.24	0.64	0.64
39N,L-10	4786	16-Mar-98	29-Mar-98	5.96	0.23	0.68	0.65
39N,L-11	4786	29-Mar-98	11-Apr-98	5.99	0.17	0.81	0.63
39N,L-12	4786	11-Apr-98	24-Apr-98	6.10	0.17	0.80	0.62
39N,L-13	4786	24-Apr-98	7-May-98	7.15	0.23	1.07	0.60
39N,L-14	4786	7-May-98	20-May-98	9.75	0.34	1.38	0.53
39N,L-15	4786	20-May-98	2-Jun-98	14.19	1.27	1.94	0.47
39N,L-16	4786	2-Jun-98	15-Jun-98	6.08	0.09	1.26	0.56
39N,L-17	4786	15-Jun-98	28-Jun-98	NA	NA	NA	NA
39N,L-18	4786	28-Jun-98	11-Jul-98	11.75	0.12	2.81	0.55
39N,L-19	4786	11-Jul-98	24-Jul-98	NA	NA	NA	NA
39N,L-20	4786	24-Jul-98	6-Aug-98	12.95	0.19	0.37	0.63
NH98 sampling interval							
39N,L-01	4752	27-Aug-98	2-Sep-98	8.94	1.00	0.67	0.61
39N,L-02	4752	2-Sep-98	20-Sep-98	12.51	0.92	1.32	0.60
39N,L-03	4752	20-Sep-98	8-Oct-98	14.71	0.72	1.64	0.68
39N,L-04	4752	8-Oct-98	26-Oct-98	13.54	0.73	0.82	0.72
39N,L-05	4752	26-Oct-98	13-Nov-98	30.41	1.85	3.11	0.71
39N,L-06	4752	13-Nov-98	1-Dec-98	13.28	0.86	0.93	0.69
39N,L-07	4752	1-Dec-98	19-Dec-98	8.56	0.55	0.45	0.69
39N,L-08	4752	19-Dec-98	6-Jan-99	12.36	0.79	0.82	0.64
39N,L-09	4752	6-Jan-99	24-Jan-99	8.90	0.62	0.75	0.68
39N,L-10	4752	24-Jan-99	11-Feb-99	6.84	0.48	0.90	0.66
39N,L-11	4752	11-Feb-99	1-Mar-99	6.16	0.56	0.60	0.62
39N,L-12	4752	1-Mar-99	19-Mar-99	4.14	0.44	0.58	0.63
39N,L-13	4752	19-Mar-99	6-Apr-99	6.07	0.46	0.83	0.57
39N,L-14	4752	6-Apr-99	24-Apr-99	6.55	0.60	0.97	0.51
39N,L-15	4752	24-Apr-99	12-May-99	22.97	1.28	15.37	0.43
39N,L-16	4752	12-May-99	30-May-99	11.55	0.65	3.23	0.45
39N,L-17	4752	30-May-99	17-Jun-99	8.02	0.65	1.37	0.53
39N,L-18	4752	17-Jun-99	5-Jul-99	13.39	1.08	1.33	0.53
39N,L-19	4752	5-Jul-99	23-Jul-99	24.08	1.98	1.66	0.56
39N,L-20	4752	23-Jul-99	10-Aug-99	21.47	1.47	1.59	0.59

A&A = alkenones and alkenoates.
NA = not analyzed because of the lack of sample.

Table 5

Name	Duration		$\delta^{13}C$ of $C_{37:2}$ MK				$\delta^{13}C$ of $C_{38:2}$MK&EK			
			No.	AV	STD	STE	No.	AV	STD	STE
NH97 sampling interval										
39N,U-01	19-Nov-97	2-Dec-97	2	-22.6	0.4	0.3	2	-21.9	0.6	0.4
39N,U-02	2-Dec-97	15-Dec-97	2	-23.3	1.1	0.8	2	-22.7	0.2	0.2
39N,U-03	15-Dec-97	28-Dec-97	2	-23.0	0.4	0.3	2	-23.3	0.0	0.0
39N,U-04	28-Dec-97	10-Jan-98	2	-22.8	0.2	0.2				
39N,U-05	10-Jan-98	23-Jan-98	2	-22.7	0.2	0.2	2	-22.1	0.5	0.4
39N,U-06	23-Jan-98	5-Feb-98	2	-22.2	0.3	0.2	2	-22.0	0.1	0.1
39N,U-07	5-Feb-98	18-Feb-98	2	-21.9	0.1	0.1	1	-23.3		
39N,U-08	18-Feb-98	3-Mar-98	2	-22.2	0.3	0.2	2	-23.8	1.3	0.9
39N,U-09	3-Mar-98	16-Mar-98	2	-22.6	0.2	0.2	1	-23.9		
39N,U-10	16-Mar-98	29-Mar-98		NA				NA		
39N,U-11	29-Mar-98	11-Apr-98	2	-23.7	0.9	0.7	1	-25.2		
39N,U-12	11-Apr-98	24-Apr-98	2	-25.9	0.6	0.4	2	-24.7	0.3	0.2
39N,U-13	24-Apr-98	7-May-98	2	-23.8	0.1	0.1	2	-22.7	0.0	0.0
39N,U-14	7-May-98	20-May-98	2	-23.3	0.4	0.3	2	-23.0	0.5	0.3
39N,U-15	20-May-98	2-Jun-98	3	-23.4	0.5	0.3	3	-23.0	0.5	0.3
39N,U-16	2-Jun-98	15-Jun-98	2	-25.2	0.1	0.1	1	-25.5		
39N,U-17	15-Jun-98	28-Jun-98	3	-25.9	2.4	1.4	1	-26.0		
39N,U-18	28-Jun-98	11-Jul-98	2	-26.5	0.6	0.4	2	-25.2	0.7	0.5
39N,U-19	11-Jul-98	24-Jul-98		NA				NA		
39N,U-20	24-Jul-98	6-Aug-98	2	-24.1	0.4	0.3	2	-24.0	0.0	0.0

No.: number of repeated measurements
AV: average
STD: standard deviation
STE: standard error.

Table 6

Sample No.	Depth cm	Age Cal. yr. BP	TOC %	OCAR mg/cm^2/ky	Alkenones μg/g	Alkenoates μg/g	Alkenone AR μg/cm^2/ky	$U^{K'}_{37}$
1	0.31	887	1.51	8.7	2.61	0.27	1.50	0.54
3	1.57	1603	1.27	7.5	0.63	0.07	0.37	0.58
5	2.83	2172	1.24	44.7	0.70	0.07	2.52	0.60
7	4.09	2293	0.82	66.0	0.85	0.09	6.88	0.60
9	5.35	2349	0.80	66.2	0.79	0.09	6.51	0.60
11	6.61	2404	0.72	61.2	1.12	0.12	9.48	0.60
15	9.12	2793	0.66	9.9	1.66	0.18	2.48	0.58
19	11.64	3459	0.78	12.2	0.98	0.03	1.54	0.63
23	14.15	4584	0.72	6.2	1.21	0.07	1.04	0.56
27	16.67	5863	0.69	6.2	1.27	0.14	1.13	0.55
31	19.19	7142	0.73	6.8	2.12	0.24	1.97	0.54
35	21.70	8421	0.87	8.5	1.94	0.23	1.89	0.52
39	24.22	9700	0.92	9.3	2.50	0.27	2.53	0.50
43	26.74	10979	0.95	10.0	2.20	0.24	2.30	0.52
Holocene average			0.91	23.1	1.47	0.15	3.01	0.57

TOC = total organic carbon
OCAR = organic carbon accumulation rate
AR = accumulation rate.

Table 7

Sampling interval	Duration	Trap position	Depth (m)	Total fine flux $mg/m^2/d$	OC $mg/m^2/d$	$CaCO_3$ $mg/m^2/d$	Opal $mg/m^2/d$	Alkenones $\mu g/m^2/d$	Alkenoates $\mu g/m^2/d$	IPT (C)	Alkenonate/Alkenone
NH97	19 November 1997 to 6 August 1998	Shallow	1366	173.45	8.15	34.65	93.52	5.21	0.05	14.3	0.010
	19 November 1997 to 10 August 1998	Middle	3056	120.29	4.87	25.80	59.16	1.80	0.04	15.7	0.022
	19 November 1997 to 6 August 1998	Deep	4786	111.25	4.28	20.57	58.54	1.15	0.04	16.5	0.032
NH98	27 August 1998 to 10 August 1999	Shallow	1332	192.55	8.83	32.54	92.51	6.57	0.19	15.3	0.029
	27 August 1998 to 10 August 1999	Middle	2472	209.03	7.68	33.73	101.58	4.11	0.16	15.5	0.039
	27 August 1998 to 10 August 1999	Deep	4752	137.22	4.75	20.74	66.84	1.95	0.13	14.5	0.065
NH97	Half depth $Z_{1/2}$			5280 m	3655 m	4474 m	5062 m	1572 m	6423 m		
	Expected at sea surface		0	198.15	9.88	42.48	104.58	8.55	0.06		
	Expected at sea bottom		5389	97.68	3.56	18.43	50.01	0.79	0.03		
NH98	Half depth $Z_{1/2}$			6215 m	3736 m	4829 m	6358 m	1982 m	5979 m		
	Expected at sea surface		0	242.50	11.66	42.65	116.86	10.15	0.22		
	Expected at sea bottom		5389	132.97	4.29	19.68	64.95	1.54	0.12		

OC = organic carbon
IPT = Integrated production temperature, defined by Conte et al. (1992).

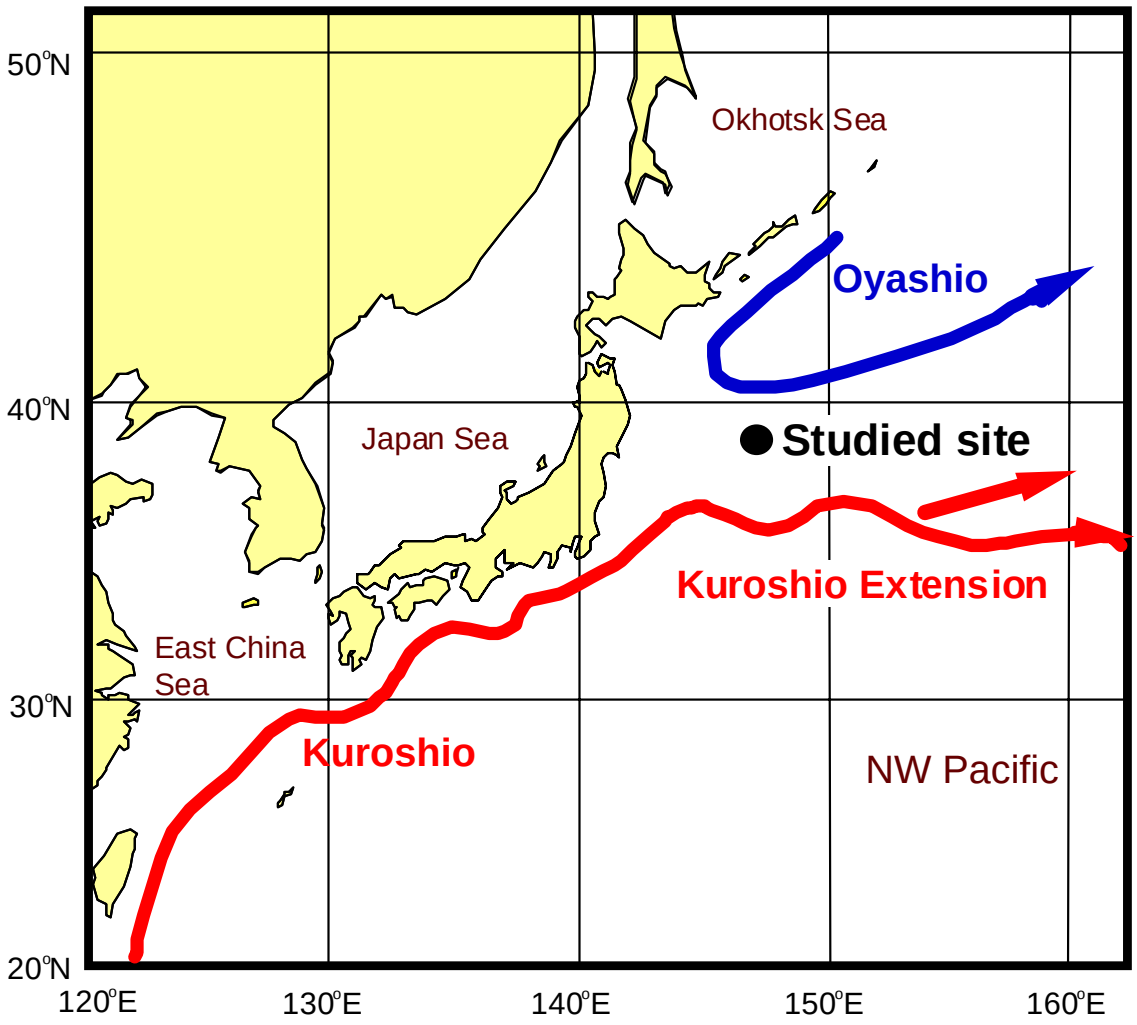
50°N
40°N
30°N
20°N
120°E
130°E
140°E
150°E
160°E
Okhotsk Sea
Oyashio
Japan Sea
Studied site
Kuroshio Extension
East China Sea
Kuroshio
NW Pacific

Fig. 1

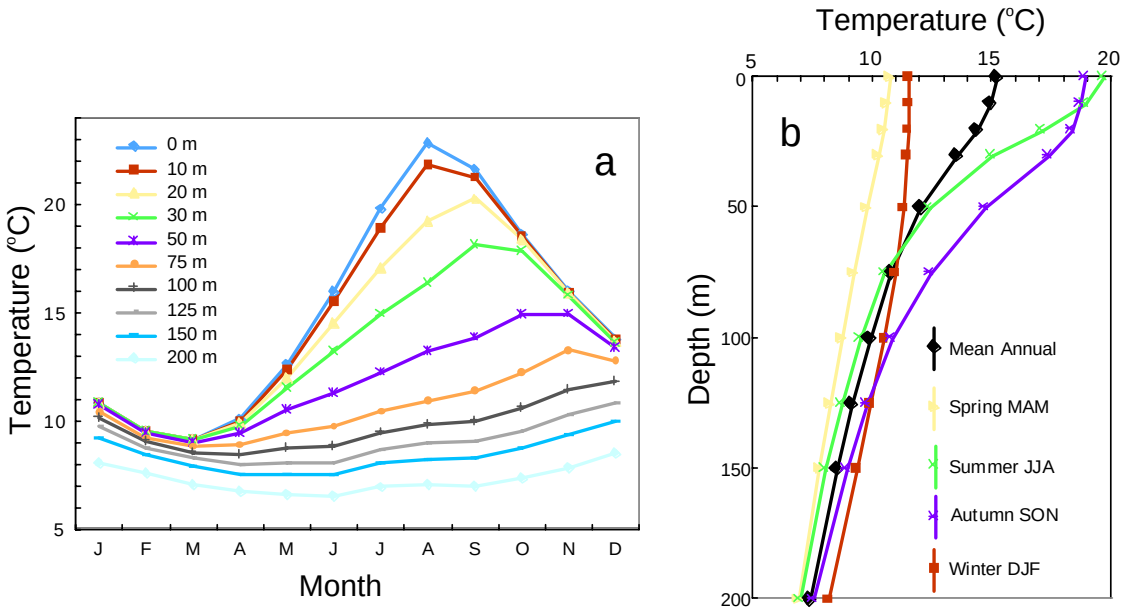
a
0 m
10 m
20 m
30 m
50 m
75 m
100 m
125 m
150 m
200 m
Temperature (°C)
Month
J F M A M J J A S O N D
5 10 15 20
b
Temperature (°C)
Depth (m)
0 50 100 150 200
Mean Annual
Spring MAM
Summer JJA
Autumn SON
Winter DJF

Fig. 2

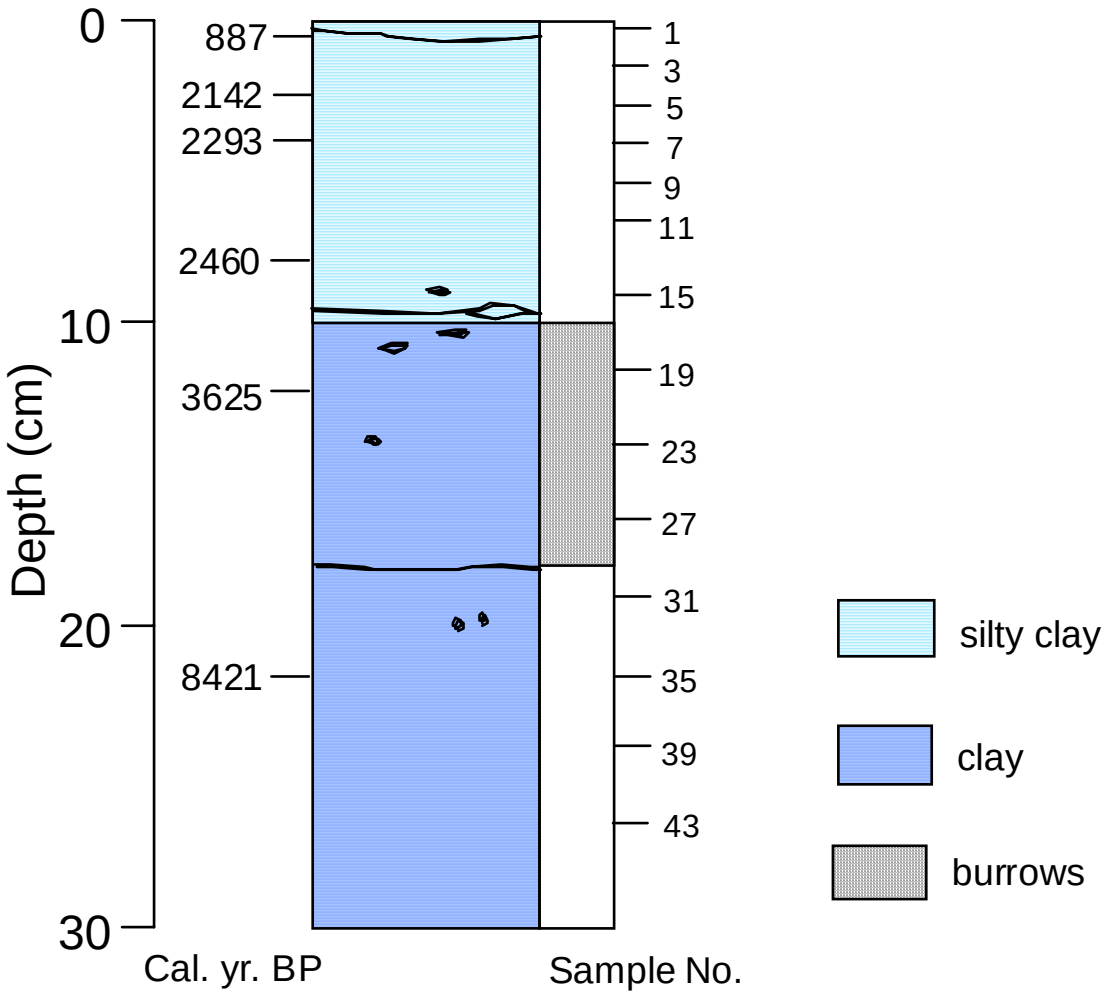
0
10
20
30
Depth (cm)
887
2142
2293
2460
3625
8421
Cal. yr. BP
1
3
5
7
9
11
15
19
23
27
31
35
39
43
Sample No.
silty clay
clay
burrows

Fig. 3

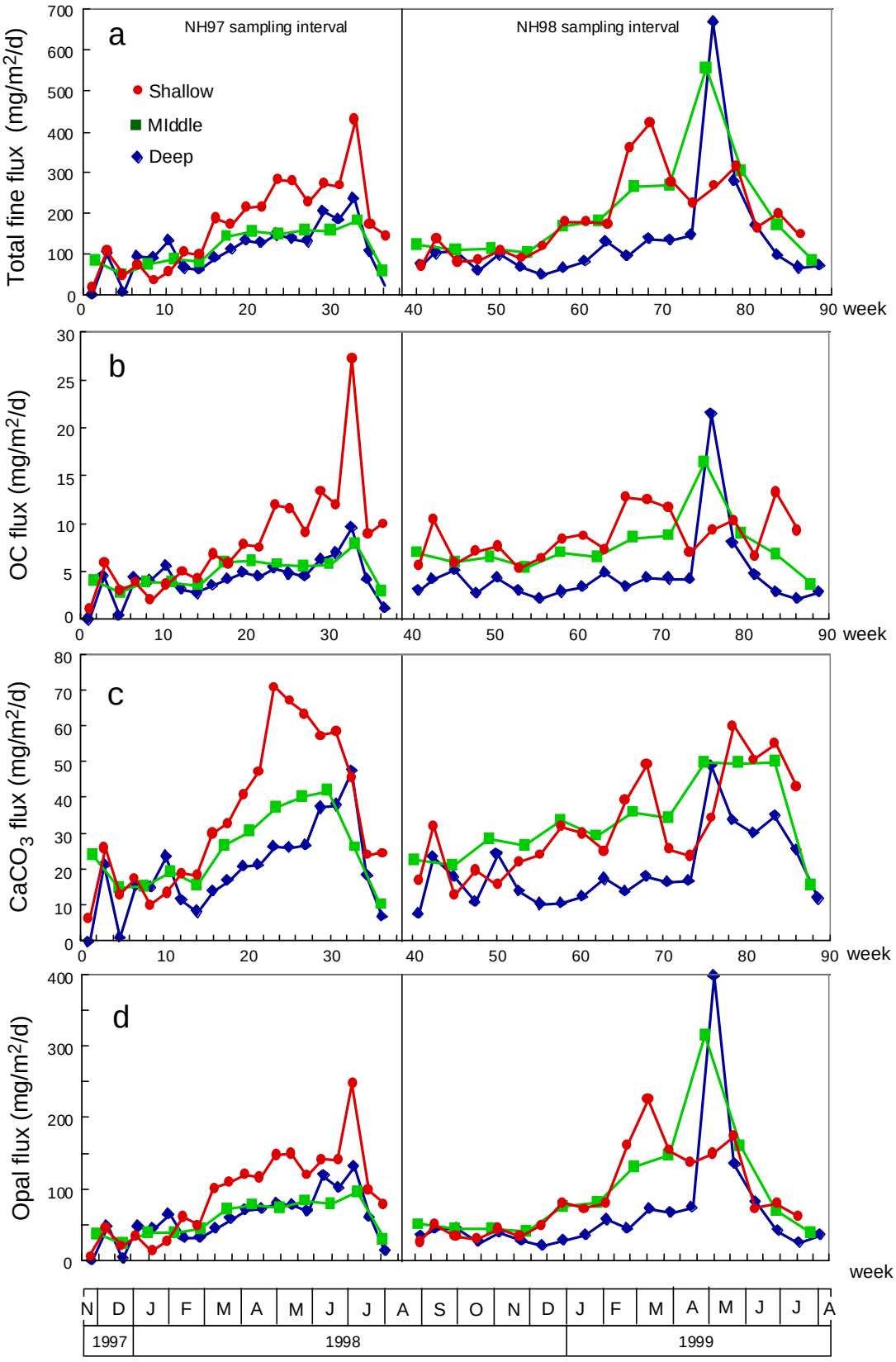
a
NH97 sampling interval
NH98 sampling interval
Shallow
MIddle
Deep
Total fine flux (mg/m2/d)
b
OC flux (mg/m2/d)
c
CaCO3 flux (mg/m2/d)
d
Opal flux (mg/m2/d)
week
N D J F M A M J J A S O N D J F M A M J J A
1997
1998
1999

Fig. 4

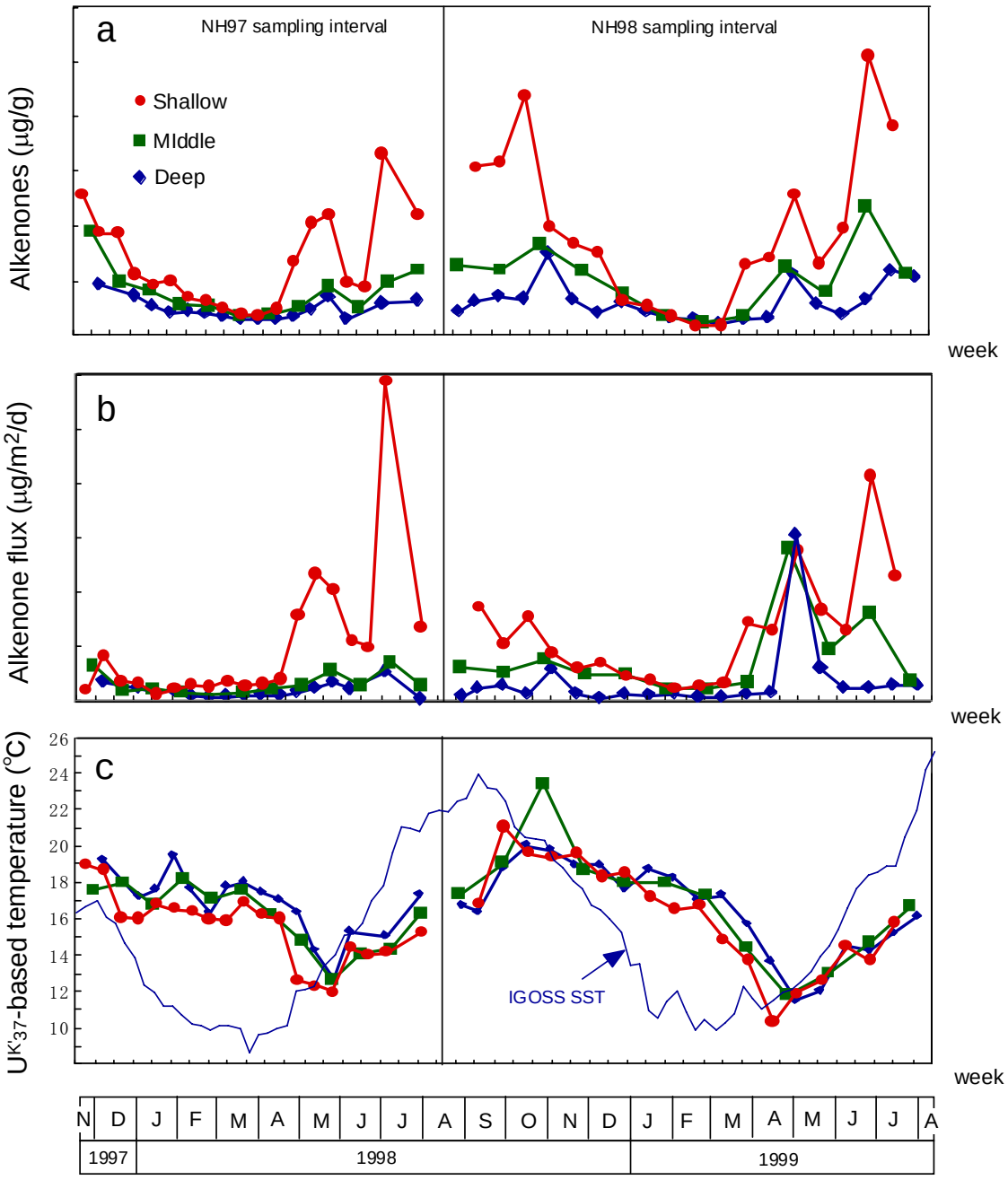
a
NH97 sampling interval
NH98 sampling interval
Shallow
MIddle
Deep
Alkenones (µg/g)
week
b
Alkenone flux (µg/m2/d)
week
c
UK'37-based temperature (°C)
26
24
22
20
18
16
14
12
10
IGOSS SST
week
N D J F M A M J J A S O N D J F M A M J J A
1997
1998
1999

Fig. 5

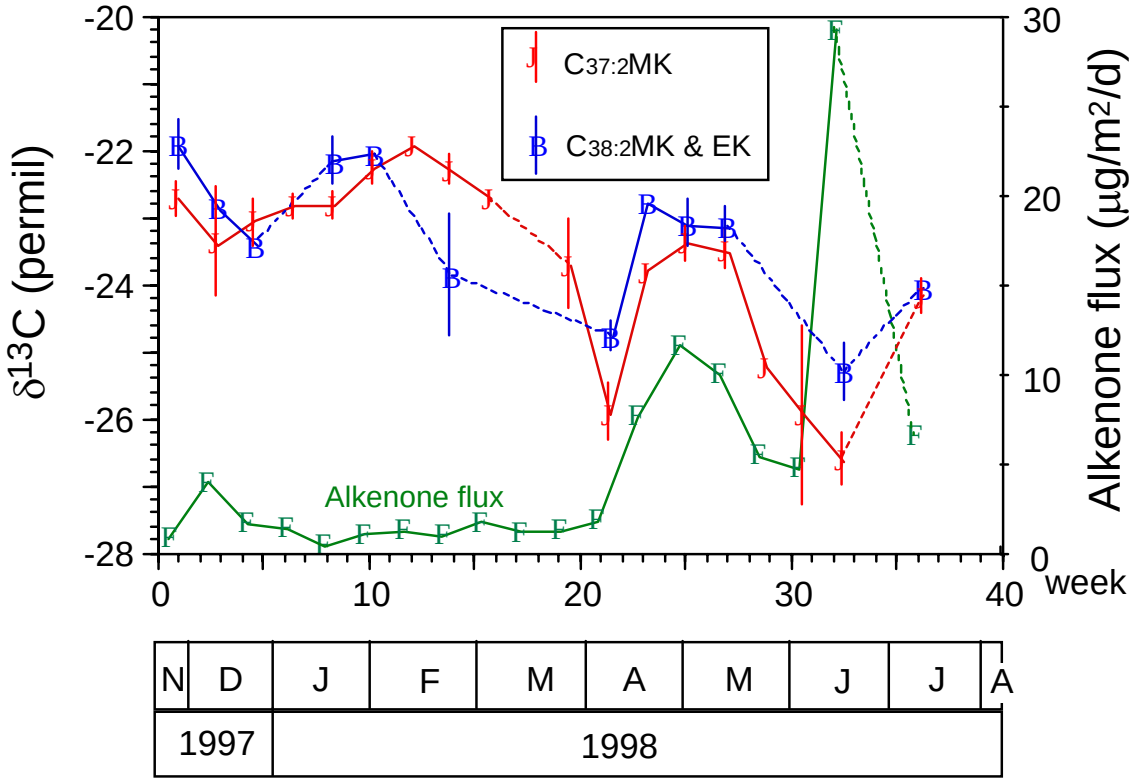
C37:2MK
C38:2MK & EK
Alkenone flux
δ13C (permil)
Alkenone flux (µg/m2/d)
week
-20
-22
-24
-26
-28
30
20
10
0
0
10
20
30
40
N
D
J
F
M
A
M
J
J
A
1997
1998

Fig. 6

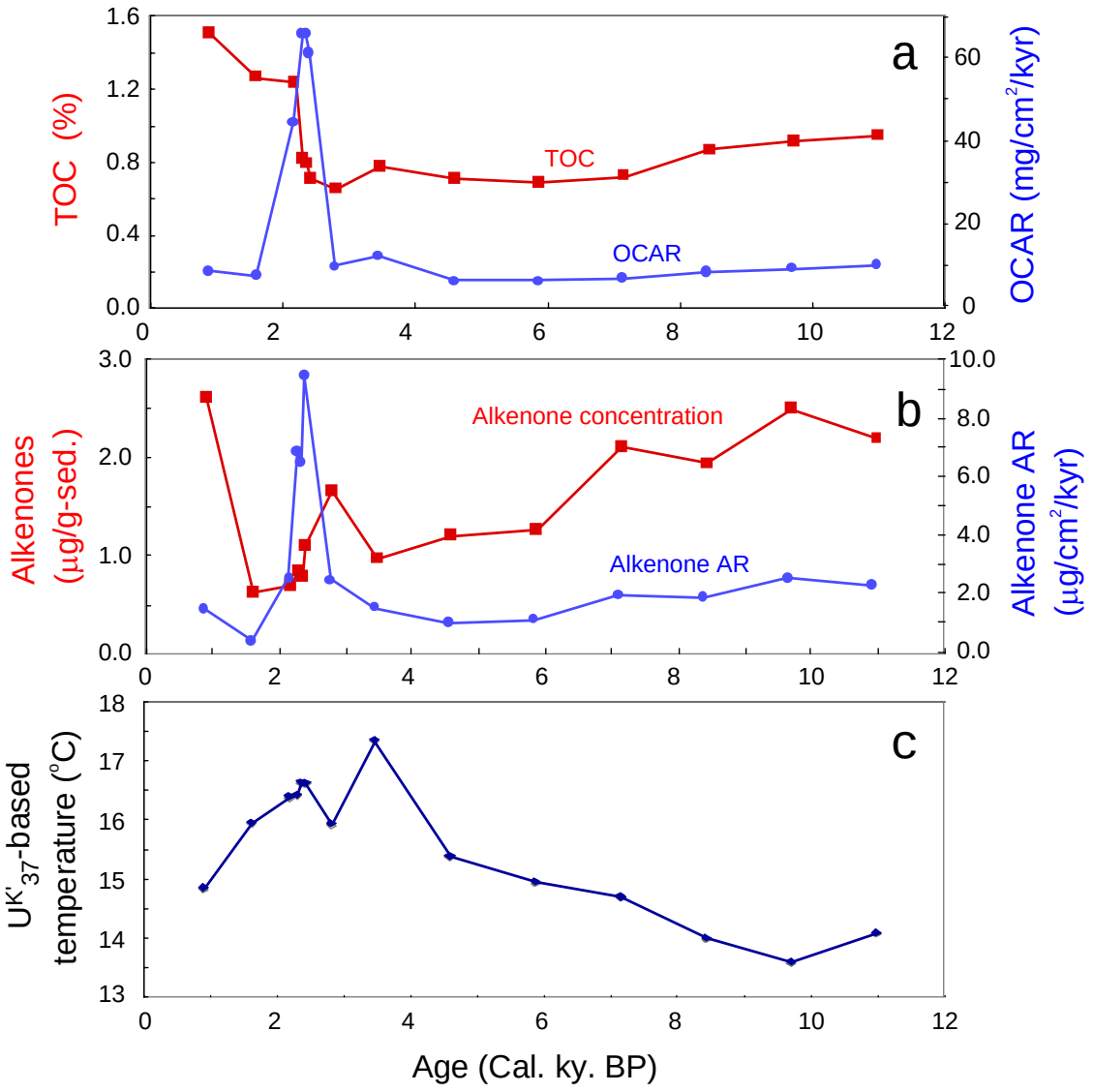
a
TOC (%)
OCAR (mg/cm²/kyr)
TOC
OCAR
b
Alkenones (µg/g-sed.)
Alkenone AR (µg/cm²/kyr)
Alkenone concentration
Alkenone AR
c
UK'37-based temperature (°C)
Age (Cal. ky. BP)

Fig. 7

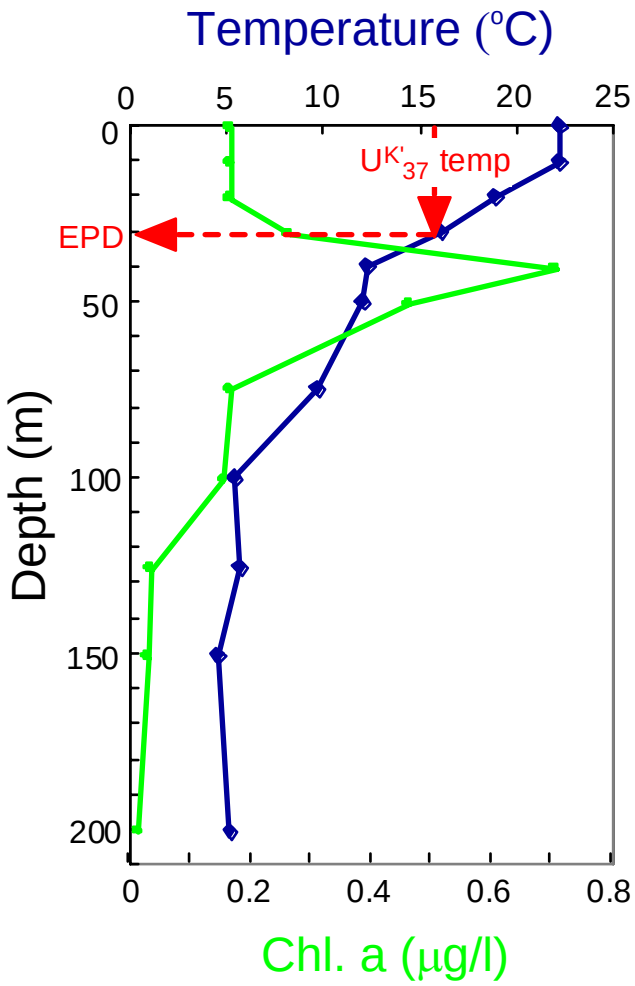
Temperature (°C)
0
5
10
15
20
25
0
50
100
150
200
Depth (m)
EPD
$U^{K'}_{37}$ temp
0
0.2
0.4
0.6
0.8
Chl. a (μg/l)

Fig. 8

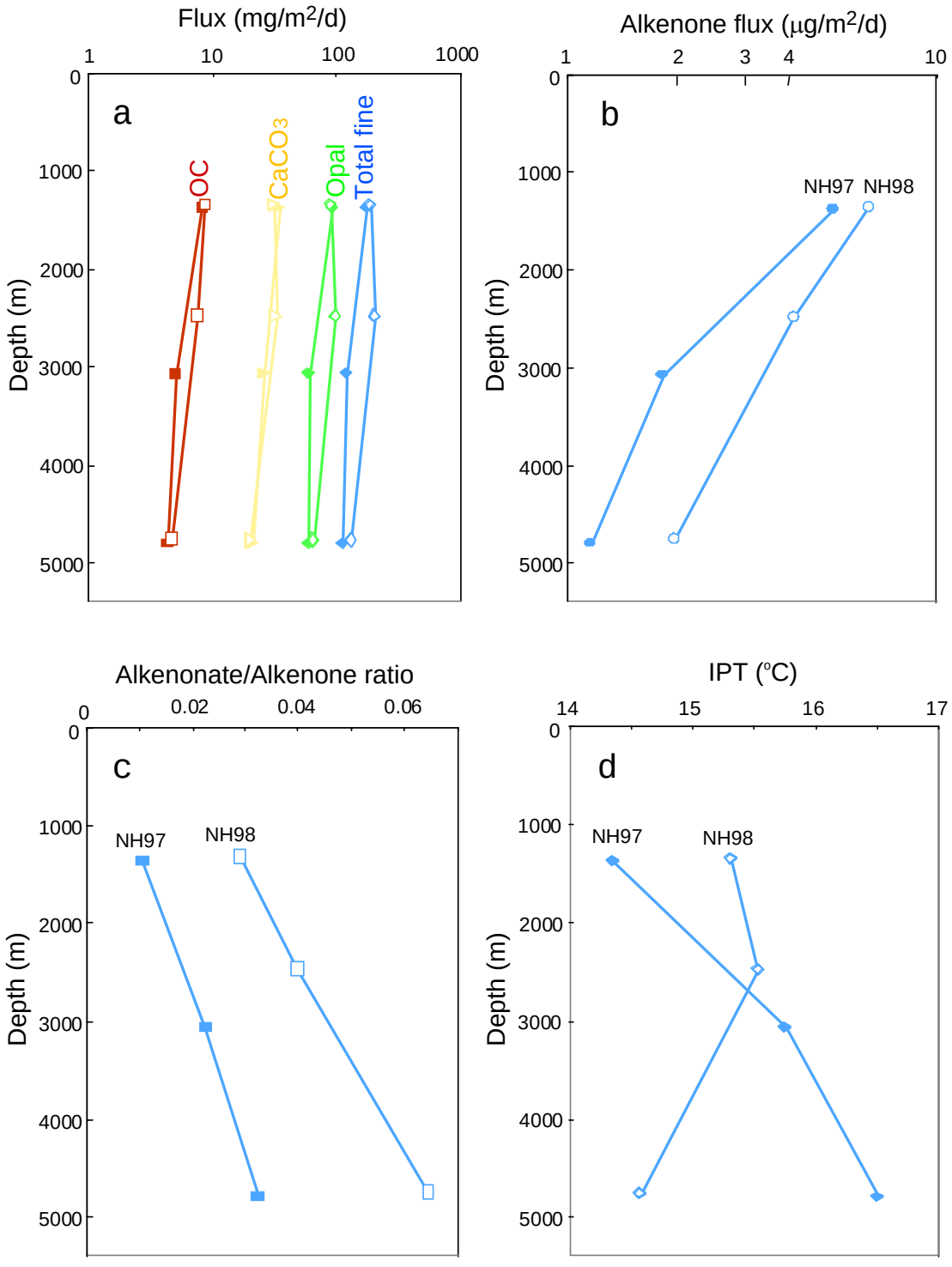
Flux (mg/m2/d)
1
10
100
1000
a
OC
CaCO3
Opal
Total fine
Depth (m)
0
1000
2000
3000
4000
5000
Alkenone flux (μg/m2/d)
1
2
3
4
10
b
NH97
NH98
Alkenonate/Alkenone ratio
0
0.02
0.04
0.06
c
NH97
NH98
IPT (°C)
14
15
16
17
d
NH97
NH98

Fig. 9

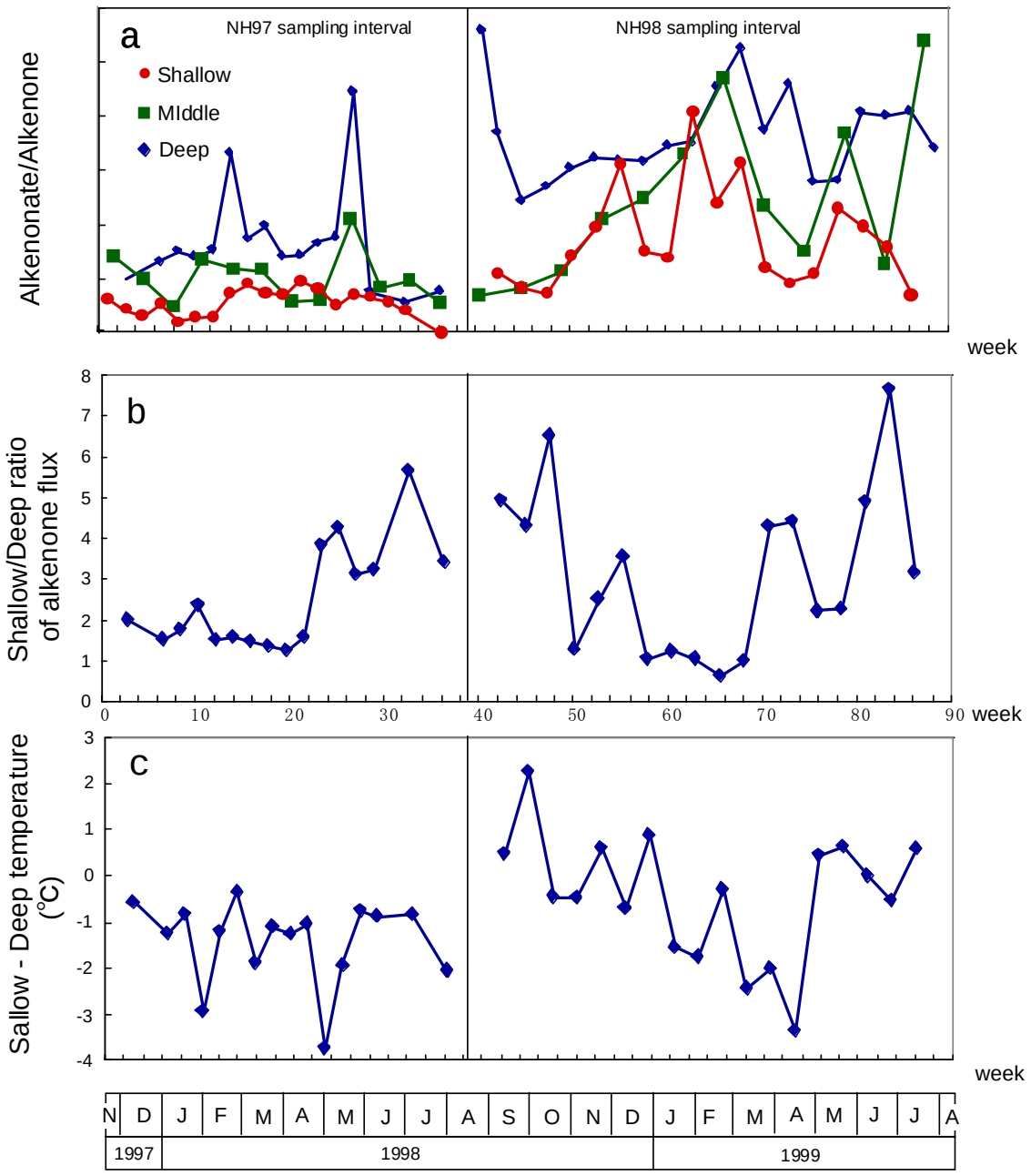
a
NH97 sampling interval
NH98 sampling interval
Shallow
MIddle
Deep
Alkenonate/Alkenone
week
b
Shallow/Deep ratio
of alkenone flux
week
c
Sallow - Deep temperature
(°C)
week
N D J F M A M J J A S O N D J F M A M J J A
1997
1998
1999

Fig. 10